Metapopulation dynamics of oysters: sources, sinks, and implications for conservation and restoration

SETH J. THEUERKAUF [iD],[1,3],† BRANDON J. PUCKETT [iD],[1,2] AND DAVID B. EGGLESTON[1]

[1]Center for Marine Sciences and Technology, Department of Marine, Earth and Atmospheric Sciences, North Carolina State University, Morehead City, North Carolina 28557 USA
[2]North Carolina Coastal Reserve and National Estuarine Research Reserve, Beaufort, North Carolina 28516 USA

Abstract. Metapopulation and source–sink dynamics are increasingly considered within spatially explicit management of wildlife populations, yet the application of these concepts has generally been limited to comparisons of the performance (e.g., demographic rates or dispersal) inside vs. outside protected areas, and at spatial scales that do not encompass an entire metapopulation. In the present study, a spatially explicit, size-structured matrix model was applied to simulate the dynamics of an Eastern oyster (*Crassostrea virginica*) metapopulation in the second largest estuary in the United States—the Albemarle-Pamlico Estuarine System in North Carolina. The model integrated larval dispersal simulations with empirical measures of oyster demographic rates to simulate the dynamics of the entire oyster metapopulation consisting of 646 reefs and five reef types: (1) restored subtidal reefs closed to harvest (i.e., sanctuaries or protected areas; *n* = 14), (2) restored subtidal reefs open to harvest (*n* = 53), (3) natural subtidal reefs open to harvest (*n* = 301), (4) natural intertidal reefs open to harvest (*n* = 129), and (5) oyster reefs on manmade, hard structures such as seawalls (*n* = 149). Key findings included (1) an overall stable, yet slightly declining oyster metapopulation, (2) variable reef type-specific population trajectories, largely dependent on spatiotemporal variation in larval recruitment, (3) a greater relative importance of inter-reef larval connectivity on metapopulation dynamics than local larval retention processes, and (4) spatiotemporal variation in the source–sink status of reef subpopulations wherein subtidal sanctuaries and reefs located in the northeastern portion of the estuary were frequent sources. From a management perspective, continued protection of oyster sanctuaries is warranted. Sanctuaries represented only 6.2% of the total reef area, however, they harbored 19% (± 2%) of all oysters and produced 25% (± 6%) of all larvae settling within the metapopulation. Additional management priorities should focus on restoration or conservation of subpopulations that serve as frequent source subpopulations (including those with poor demographic rates, but high connectivity potential), and management of harvest from sink subpopulations. The application of a source–sink framework and similar integrated modeling approach could inform management of oysters in other systems, as well as other species that exhibit similar metapopulation characteristics.

[3]Present address: Office of Aquaculture, National Marine Fisheries Service, National Oceanic and Atmospheric Administration, Silver Spring Maryland 20910 USA.
† **E-mail:** Seth.Theuerkauf@noaa.gov

INTRODUCTION

Metapopulation concepts—wherein subpopulations are viewed as interconnected networks with asynchronous demographic (i.e., birth, death) and dispersal rates (i.e., immigration, emigration)—are a critical underpinning of spatially explicit conservation and restoration of wildlife populations (Beissinger and Westphal 1998, Hanski 1998, Burgess et al. 2014, Seward et al. 2018). The application of metapopulation concepts is particularly important in cases where the management of wildlife populations is multifaceted, such that parts of the population are either harvested, located inside protected areas, or undergoing restoration (Puckett and Eggleston 2016). The application of metapopulation concepts to spatial management has often taken the form of comparisons (e.g., demographic rates or dispersal) inside vs. outside protected areas (e.g., Crowder et al. 2000). Rarely is the performance of protected areas or other managed subpopulations considered within the broader context of the entire metapopulation, wherein dynamics are simulated within and among all subpopulations. Comprehensive evaluation of metapopulation dynamics is needed to inform spatial management of populations such that disparate management strategies (e.g., protected areas, harvest, and restoration) can be integrated and evaluated within a single framework.

Demographic rates (births and deaths) and dispersal rates (emigration and immigration) drive metapopulation dynamics (Pulliam 1988, Hanski 1998). In marine systems, the relative importance of demographic rates to metapopulation dynamics is poorly understood because demographic rates can become decoupled from recruitment due to open subpopulations interconnected via pelagic larval dispersal (hereafter referred to as larval connectivity; Planes et al. 2009). Thus, understanding the drivers of metapopulation dynamics in marine systems requires knowledge of both demographic rates and the direction and magnitude of larval connectivity among subpopulations, including the degree of local larval retention (i.e., larvae recruiting to their natal subpopulation) vs. larval export (i.e., larvae recruiting to a non-natal subpopulation; Kritzer and Sale 2006 and references therein). When rates of local larval retention are

low and larval export is high, the importance of subpopulation demographics on metapopulation dynamics diminishes as recruitment at a subpopulation is decoupled from its reproduction (Warner and Cowen 2002, Figueira 2009). Conversely, as local larval retention increases (e.g., subpopulations are more isolated), local demographics often become increasingly important to metapopulation dynamics (Figueira 2009, Carson et al. 2011, Puckett and Eggleston 2016).

Source–sink dynamics, wherein the balance between subpopulation demographic and dispersal rates determines source and sink subpopulations, are a key component of the metapopulation concept (Pulliam 1988). Source subpopulations are generally in areas of high habitat quality where birth rates exceed death rates and may be located—in the case of marine systems—in areas where prevailing currents deliver disproportionate amounts of larvae to other subpopulations. Source subpopulations contribute disproportionately to metapopulation persistence. Sink subpopulations are generally in areas of reduced habitat quality where death rates exceed birth rates—often leading sink subpopulations toward extinction unless subsidized by sufficient emigrants from other subpopulations. Source–sink status is generally nonbinary and can fluctuate temporally depending upon local conditions. For example, variation in local water current direction and magnitude can either isolate or connect subpopulations of coral reef-associated fish (Bode et al. 2006, Figueira 2009). An understanding of spatiotemporal variation in source–sink dynamics of subpopulations is essential to the effective management of wildlife metapopulations, wherein management efforts generally attempt to protect or restore source subpopulations and manage harvest from sink subpopulations.

Metapopulation and source–sink dynamics are increasingly considered within the context of management for sessile marine species such as corals and oysters, wherein subpopulations are only connected via larval dispersal (Botsford et al. 2003, Figueira and Crowder 2006, Burgess et al. 2014, Holstein et al. 2015, Puckett and Eggleston 2016). These systems are particularly amenable to testing metapopulation and source–sink concepts because of (1) the presence of spatially separated subpopulations (i.e., reefs), (2) spatiotemporal variation in spawning (Hughes et al. 2000, Mroch et al. 2012),

(3) spatiotemporal variation in demographic rates such as fecundity, growth, and survival (Mroch et al. 2012, Puckett and Eggleston 2012, Peters et al. 2017, Theuerkauf et al. 2017), and (4) variation in potential larval connectivity due to hydrodynamics that vary with synoptic-scale forcing such as wind (Cowen et al. 2000, Haase et al. 2012, Puckett et al. 2014, Kroll et al. 2018).

In the present study, a spatially explicit, size-structured, discrete-time matrix metapopulation model originally developed by Puckett and Eggleston (2016) for Eastern oysters (*Crassostrea virginica*) within a network of no-take reserves was expanded to simulate the dynamics of an oyster metapopulation in the Albemarle-Pamlico Estuarine System in North Carolina, USA. The model integrated larval dispersal simulations with empirical measures of oyster demographic rates to simulate the dynamics of the entire oyster metapopulation consisting of 646 reefs and five reef types: (1) restored subtidal reefs closed to harvest (i.e., sanctuaries or protected areas; $n = 14$), (2) restored subtidal reefs open to harvest ($n = 53$), (3) natural subtidal reefs open to harvest ($n = 301$), (4) natural intertidal reefs open to harvest ($n = 129$), and (5) oyster reefs on manmade, hard structures such as seawalls ($n = 149$). The metapopulation model was used to estimate (1) overall metapopulation trends, (2) reef type- and size class-specific population trajectories, (3) the degree and relative importance of local larval retention and inter-reef connectivity on metapopulation dynamics, and (4) spatiotemporal variation in source–sink structure within this metapopulation. We addressed the following general questions via the metapopulation model framework: (1) What is the relative importance of no-harvest sanctuary oyster reefs to the overall metapopulation? (2) Is there consistency in source–sink structure in space and time that could inform conservation and management? and (3) Are metapopulation dynamics driven more by inter-reef larval export or local larval retention processes and associated subpopulation (i.e., reef) demographic rates?

METHODS

Study system

The Albemarle-Pamlico Estuarine System (APES) in North Carolina contains (from north to south) Albemarle, Pamlico, and Core Sounds. The APES is the largest lagoonal estuary in the United States and is bounded by a barrier island chain that limits exchange with the coastal ocean to five relatively small inlets (~1 km wide; Fig. 1; Pietrafesa et al. 1986). Tides in and near the inlets of the APES are generally semi-diurnal, with a mean vertical range of 5 cm when averaged across Pamlico Sound (Roelofs and Bumpus 1953) to 30 cm in Core Sound (Dudley and Judy 1973). The APES is relatively shallow with a mean depth of ~4.5 m and a maximum depth of 7.5 m (Epperly and Ross 1986). Water circulation patterns within the APES are due predominately to wind-driven currents and riverine freshwater input, with an increasing tidal influence from north to south (Xie and Eggleston 1999). Circulation during the summer, when primary and secondary peaks in oyster spawning occur (Mroch et al. 2012), is driven predominately by south-westerly winds (Puckett and Eggleston 2012). These winds derive from synoptic-scale frontal systems that transverse the region (Pietrafesa et al. 1986). Wind patterns in the region have a strong influence on spatiotemporal variation in larval dispersal patterns of oysters (Haase et al. 2012, Puckett et al. 2014).

Study species

Eastern oysters (*Crassostrea virginica*, hereafter oysters) are distributed throughout estuaries along eastern North America, ranging from the Gulf of St. Lawrence to the Gulf of Mexico, and provide a multitude of ecosystem services within estuaries, such as water filtration, sediment stabilization, and essential fish habitat (Kennedy et al. 1996, Coen et al. 2007, Grabowski and Peterson 2007, Pierson and Eggleston 2014). Oysters form dense, three-dimensional reef structures that are connected via larval dispersal, whereby sessile individuals spawn gametes into the water column and fertilized eggs develop into planktonic larvae that are distributed via currents (Kennedy et al. 1996). After a two- to three-week period, larvae seek hard structures on the benthos for permanent settlement.

Multiple natural and restored oyster reef types exist within the subtidal and intertidal zones of the APES (Fig. 1). Within the subtidal zone, there are (1) commercially harvested natural oyster reefs, (2) commercially harvested reefs restored
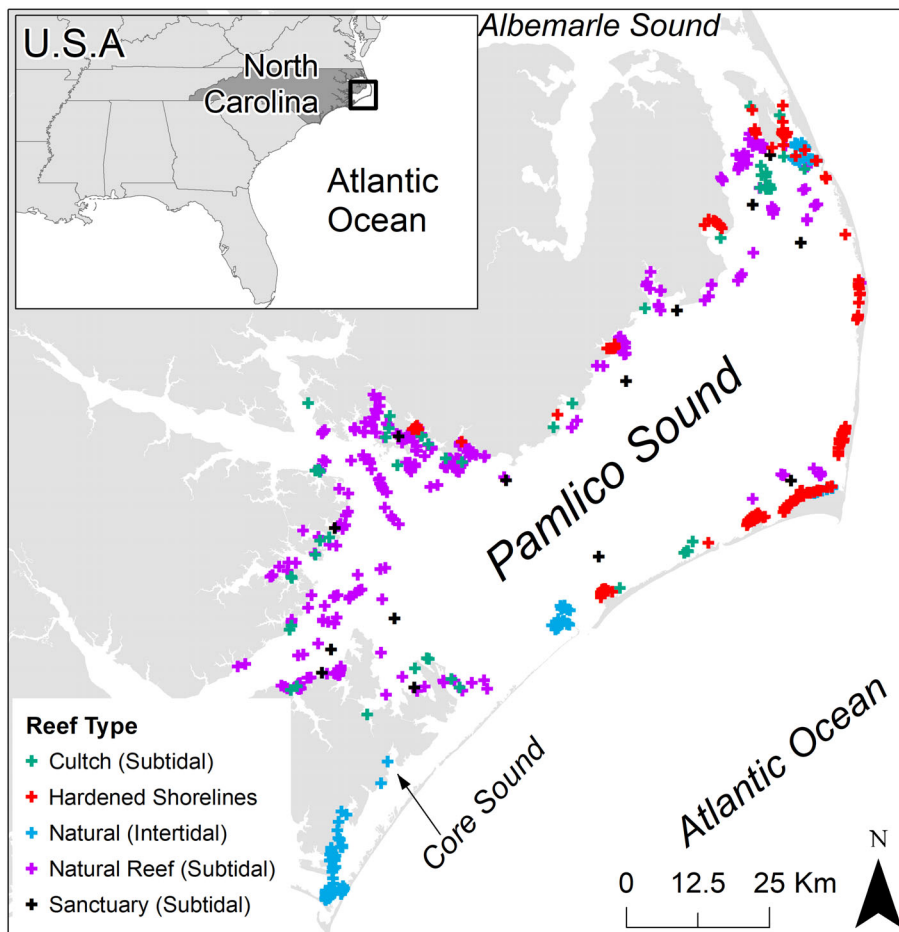
Fig. 1. Map of the Albemarle-Pamlico Estuarine System showing the distribution of various oyster reefs by reef type, including cultch (teal), hardened shorelines (red), natural intertidal (blue), natural subtidal (purple), and sanctuary (black) reefs. Reefs not to scale.

with shell, concrete, or limestone-marl reef substrates (i.e., cultch reefs), and (3) reefs restored with high vertical relief and protected from commercial harvest (i.e., sanctuaries; Puckett and Eggleston 2012, Peters et al. 2017). Within the intertidal zone, oysters exist on (4) natural reefs and (5) hardened shoreline structures, such as bulkhead and riprap revetments (Theuerkauf et al. 2016, 2017). All reefs exist within a salinity range of approximately 10–36 psu and are separated from each other by <1–125 km.

General modeling approach

Our general modeling approach incorporated (1) the spatial distribution and areal footprint of all oyster reef types within the APES, (2) reef type- and intra-annual-specific oyster size-class transition probabilities (i.e., probability of surviving and remaining in a given size class or surviving and growing into the next size class; sensu Caswell 2001), (3) size-specific oyster fecundity estimates, and (4) local larval retention and inter-reef connectivity via larval dispersal simulations. With this modeling approach, metapopulation dynamics throughout the APES were simulated using a demographic matrix model over a five-year time period (2012–2016), which generally overlapped with collection of empirical demographic and validation data, and allowed for evaluation in consistency of

metapopulation source–sink structure over space and time.

Estimating reef footprints

Multiple geospatial data sources were integrated to generate estimates of oyster reef areal footprints for all reef types within the APES. All natural and restored (i.e., cultch planting and sanctuary) oyster reef footprints were provided as map layers by the North Carolina Division of Marine Fisheries Shellfish Mapping Program (North Carolina Department of Environmental Quality and Division of Marine Fisheries 2013), and were adjusted where appropriate based on ground truth surveys conducted by Peters et al. (2017) and Theuerkauf et al. (2016). For a more detailed description of methods used to adjust subtidal reef areal footprints, refer to Peters et al. (2017), and for adjustment of intertidal reef areal footprint, refer to Theuerkauf et al. (2016). Subtidal natural oyster reef footprints were further adjusted based on live oyster density data collected by the North Carolina Division of Marine Fisheries Shellfish Mapping Program from 2007 to 2009. It is important to note that the original map layers provided by the North Carolina Division of Marine Fisheries Shellfish Mapping Program included a range of shell habitat quality from areas of loose shell fragments containing no live oysters, to scattered, low-density assemblages of oysters, to high-density oyster reefs (Theuerkauf et al. 2017). Adjustment of these map layers was required to ensure the distribution of reef footprints considered in subsequent modeling reflected the distribution of oyster reefs with densities >10 m^{-2} (i.e., minimum density criterion to define a reef; sensu Powers et al. 2009, Theuerkauf et al. 2016). The distribution of hardened shorelines from map layers included all areas of bulkhead and riprap revetments installed prior to 2012 and were provided by the North Carolina Division of Coastal Management Estuarine Shoreline Mapping Program (North Carolina Department of Environmental Quality and Division of Coastal Management 2012). Map layers of hardened shoreline structures were adjusted to reflect the distribution of structures with oyster densities >10 m^{-2} based on ground truthing (Theuerkauf et al. 2016). A total of 646 reefs were identified and utilized in the present study. Table 1 provides summary statistics by reef type including number of unique reefs, total

Table 1. Summary information on number of unique reefs, total reef area, average reef area, average initial density (ind. m^{-2}), average initial population size, and average initial size structure by reef type for model simulations.

| Reef type | No. of unique reefs | Total reef area (ha) | Average reef area (ha) | Average initial density (ind. m^{-2}) | Average initial population size (% of metapopulation) | Average initial size structure (% in size class) | | |
						Recruits (0–30 mm)	Subadults (30–75 mm)	Adults (75 mm+)
Subtidal natural reefs	301	934.27	3.12	61	2,307,464	29	55	16
Subtidal cultch reefs	53	15.32	0.29	152	438,967	28	54	18
Subtidal sanctuary reefs	14	66.02	4.72	670	26,323,847	25	68	7
Hardened shoreline reefs	149	2.69	0.10	69	69,653	2	65	33
Intertidal natural reefs (Pamlico Sound)	57	10.43	0.28	121	384,183	34	58	8
Intertidal natural reefs (Core Sound)	72	11.82	0.24	842	2,483,700	39	55	6

Notes: Reef location and area information were derived from the North Carolina Division of Marine Fisheries Shellfish Mapping Program and the North Carolina Division of Coastal Management Estuarine Shoreline Mapping Program. Average initial densities for each reef type were derived from Peters et al. (2017), Theuerkauf et al. (2017) and Puckett and Eggleston (2016). Average initial population size was calculated by multiplying spatially explicit oyster densities m^{-2} by reef area. Average initial size structure represents the average percentage of individuals within a given size class on a given reef used to initialize the metapopulation model.

reef area, average reef area, average initial density, average initial population size, and average initial size structure. Fig. 1 displays the spatial distribution of these reefs within the APES by reef type.

Estimating demographic rates via field sampling

Oyster density and length frequency were quantified on a subset of subpopulations of all reef types via repeated field sampling of existing reefs (two to three samplings per year, coinciding with the timing of major recruitment events, over a two- to three-year time period) using comparable methods between 2006 and 2015. Puckett and Eggleston (2012) sampled no-harvest oyster sanctuaries ($n = 6$, three samplings per year, 2006–2008), Peters et al. (2017) sampled subtidal natural reefs ($n = 8$, three samplings per year, 2011–2013) and cultch reefs ($n = 16$, three samplings per year, 2011–2013), and Theuerkauf et al. (2017) sampled intertidal natural reefs ($n = 16$, three samplings per year, 2014–2015) and hardened shoreline structures ($n = 19$, two samplings per year, 2014–2015). The subset of subpopulations examined for all reef types spanned the length–width axis of the APES ~ 7800 km². Oyster density and length frequency were quantified on reefs randomly selected from maps of existing reefs via random quadrat sampling (0.25–1 m²). The number of quadrat samples collected per reef was proportional to reef area. Quadrat samples for subtidal oyster reefs were obtained via SCUBA divers. It is important to note that in addition to random quadrat sampling of oyster sanctuaries, Puckett and Eggleston (2012) conducted a mark–recapture study of oysters to validate growth and survival rates as estimated via random quadrat sampling and cohort analyses. These mark–recapture data were used to develop the method described below for utilizing size structure data collected via quadrats from the oyster subpopulations examined in the APES, which was used to estimate growth and survival transition probabilities, a necessary component of demographic matrix modeling to estimate growth and mortality. Size class-specific densities observed at the first sampling of a given reef type were also used to parameterize the demographic matrix model with an initial population estimate for all reefs. Specifically, observed density estimates (individuals m^{-2}) were interpolated via ordinary kriging (Esri 2016) among sampled locations to predict reef type-specific oyster densities across the APES. Predicted oyster density estimates for nonsampled reef locations were then extracted from these continuous, interpolated data and multiplied by reef area to generate initial population estimates for each reef considered within the model domain (Fig. 1).

Estimating growth and survival transition probabilities

Field-derived, oyster size structure data were used to estimate reef type- and intra-annual-specific growth and survival transition probabilities. Specifically, for each reef type, oyster density data were averaged from all quadrats for a given reef site for each sampling event and subsequently partitioned into three size classes: (1) recruit (LVL < 30 mm), (2) subadult (30 mm ≤ LVL < 75 mm), and (3) adult oysters (LVL ≥ 75 mm; legally harvestable size). A linear optimization approach was used to determine the least-squares estimate for five growth and survival transition probabilities based on size class-specific density data from time t and $t + 1$. These five transition probabilities included the probability of surviving and remaining in a size class (i.e., recruit at t to recruit at $t + 1$, subadult at t to subadult at $t + 1$, adult at t to adult at $t + 1$), and the probability of surviving and growing into larger size classes (i.e., recruit at t to subadult at $t + 1$, subadult at t to adult at $t + 1$; sensu Caswell 2001). To predict least-squares size class-specific density estimates at $t + 1$ and minimize the total sums of square difference between predicted and observed densities for the three size classes at $t + 1$, linear optimization was used to adjust the five transition probabilities that were multiplied by the observed size class-specific densities at t and summed where appropriate. As transition probabilities cannot exceed 1 (equivalent to 100% survival), and cannot be less than 0 (e.g., 0% survival), initial constraints within the linear optimization for each of the five transition probabilities were applied as 0.01 and 0.99. The sum of the recruit at t to recruit at $t + 1$, as well as that for the recruit at t to subadult at $t + 1$, the subadult at t to subadult at $t + 1$, and the subadult at t to adult at $t + 1$, were constrained to be no greater than 1.

The efficacy of this method was evaluated by comparing season-specific transition probabilities determined empirically from a mark–recapture study used previously to characterize transition probabilities for subtidal oyster sanctuary reefs (see Puckett and Eggleston (2012) for description of methods), with those estimated using the linear optimization method described above. The same field-derived size structure data for subtidal sanctuaries in the APES from Puckett and Eggleston (2012) were used in both methods, providing a standardized basis for comparison. Initial comparison of these transition probabilities identified that linear optimization with wide constraints for each possible transition probability (i.e., 0.01–0.99) resulted in underestimates of various transition probabilities relative to those determined from the mark–recapture study. Thus, we subsequently modified the constraints within the linear optimization for all recruit and sublegal transitions to reflect the minimum and maximum observed values for transition probabilities from the mark–recapture study (i.e., empirically derived spatially and season-specific transition probabilities for six oyster sanctuaries in the APES; Puckett and Eggleston 2016). This resulted in narrower constraints for the various transition probabilities within the linear optimization approach and yielded an improved fit of estimated transition probabilities derived from the mark–recapture study (Appendix S1: Fig. S1). Since the intent was to develop a universal method for using linear optimization to estimate transition probabilities for all reef types within our study system, we did not constrain the adult transition (i.e., adult at t to the adult at $t + 1$) using minimum and maximum observed values as harvest is not prohibited from other subpopulations other than those located in no-take sanctuaries. We also developed unique transition probability estimates for intertidal natural reefs in Core vs. Pamlico Sounds since prior research indicated significant differences in density and demographic rates between water bodies (Theuerkauf et al. 2017). A summary of reef type- and season-specific oyster growth and survival transition probabilities used in model simulations is included in Table 2.

Estimating fecundity

Size-specific oyster fecundity was estimated from a previous study that quantified size class-specific mean total egg content (i.e., per capita fecundity) of oysters (Mroch et al. 2012). Fecundity estimates were generated from this dataset for three size classes, that is, 0–30 mm (recruit), 30–75 mm (subadult), and 75+ mm (adult). Specifically, randomly selected oysters ($n = 2067$) were collected from six reef sites throughout the APES during May and August 2006–2007. Oysters were processed individually to determine per capita fecundity following the general procedures in Cox and Mann (1992). Mean per capita fecundity was calculated for each oyster size class across six reef sites to generate a mean per capita fecundity for each of the three size classes, and temporally corresponding with the primary and secondary peaks in oyster reproductive output for the APES (i.e., May–June and July–August; Table 3). Males were included in the calculations of mean per capita fecundity, thereby incorporating the sex ratio of a given size class. For a more detailed description of fecundity methods, see Mroch et al. (2012).

Estimating larval connectivity

A coupled hydrodynamic and particle tracking model that was validated was used to quantify local larval retention and inter-reef larval connectivity (Luettich et al. 2002, Haase et al. 2012, Puckett et al. 2014). The hydrodynamic model was forced with hourly wind velocities measured from May through August 2012–2016 at Cape Hatteras Meteorological Station. Water current velocities were output from the model at hourly intervals following an eight-day model spin-up. A total of 813,960 particles were tracked, including release of nine particles from evenly spaced grid nodes within each of 646 reefs at 24-h intervals over a 14-d period in late May and late July of each year to coincide with the primary and secondary peaks in oyster reproductive output in the APES (i.e., 252 particles/reef/year for a total of 1260 particles/reef). Particles (hereafter "larvae") were assumed to be passive surface drifters and subjected to predicted surface currents. Previous research in this shallow, well-mixed system revealed that connectivity was driven primarily by location of natal reef, date of spawning, and their interaction—larval behavior and the number of larvae released were of secondary importance (Puckett et al. 2014, Puckett and Eggleston 2016). Moreover, as described above, the APES is a shallow, wind-

Table 2. Reef type- and seasonally specific transition probabilities utilized in model simulations.

| | Stage at t | | | | | | | | |
| | May–June (spring) | | | July–August (summer) | | | September–April (fall/winter) | | |
Stage at $t + 1$	Recruits	Subadults	Adults	Recruits	Subadults	Adults	Recruits	Subadults	Adults
Natural (subtidal)									
Recruits	0.21	0	0	0.23	0	0	0.16	0	0
Subadults	0.29	0.70	0	0.58	0.65	0	0.38	0.49	0
Adults	0	0.08	0.58	0	0.01	0.22	0	0.23	0.07
Cultch (subtidal)									
Recruits	0.21	0	0	0.23	0	0	0.21	0	0
Subadults	0.29	0.61	0	0.58	0.65	0	0.38	0.49	0
Adults	0	0.01	0.62	0	0.08	0.23	0	0.08	0.06
Sanctuary (subtidal)									
Recruits	0.1	0	0	0.11	0	0	0.11	0	0
Subadults	0.45	0.71	0	0.73	0.72	0	0.08	0.71	0
Adults	0	0.1	0.87	0	0.11	0.79	0	0.49	0.04
Hardened shorelines									
Recruits	0.21	0	0	0.08	0	0	0.21	0	0
Subadults	0.29	0.61	0	0.92	0.65	0	0.38	0.77	0
Adults	0	0.04	0.65	0	0.03	0.38	0	0.21	0.99
Natural (intertidal, Core Sound)									
Recruits	0.21	0	0	0.23	0	0	0.21	0	0
Subadults	0.29	0.61	0	0.58	0.77	0	0.42	0.49	0
Adults	0	0.05	0.68	0	0.01	0.36	0	0.09	0.01
Natural (intertidal, Pamlico Sound)									
Recruits	0.21	0	0	0.23	0	0	0.21	0	0
Subadults	0.29	0.61	0	0.77	0.77	0	0.71	0.77	0
Adults	0	0.02	0.99	0	0.02	0.99	0	0.02	0.01

Note: Transition probabilities represent the probability of surviving and remaining in a given size class or surviving and growing into the next size class (sensu Caswell 2001).

Table 3. Size class-specific (i.e., 0–30 mm, 30–75 mm, and 75+ mm) and seasonally explicit (i.e., May–June and July–August) per capita oyster fecundity estimates (no. of eggs/oyster) for oyster reefs in APES used in metapopulation simulations (derived from Mroch et al. 2012).

| | Season | |
Size class	May–June	July–August
0–30 mm	345.98	51.92
30–75 mm	7166.70	472.35
75+ mm	37,333.25	1737.92

driven lagoonal estuary with a well-mixed water column and no distinct halocline for much of the year (Reyns et al. 2007). Larvae were tracked hourly over a 21-d larval duration. As described in more detail below, three proportional daily larval mortality rates were applied: 7.5%, 10%, and 20% d^{-1} to three unique metapopulation model scenarios based on literature-derived relationships between larval duration and mortality (Mann and Evans 1998). Larvae were assumed competent to settle from day 14 through day 21, after which larvae remaining in the water column died (e.g., North et al. 2008, Puckett and Eggleston 2016). Settlement was assumed to occur if larvae that were competent to settle were located within reef polygon boundaries.

Oyster metapopulation connectivity matrices were generated for May–June and July–August 2012–2016 (i.e., 2 matrices/year × 5 yr = 10 connectivity matrices). Matrix elements represent the proportion of larvae released from a row-referenced reef that settled in a column-referenced reef. Local retention—the probability of larvae spawned from a reef returning to settle within their natal reef—was obtained from the diagonal elements of the connectivity matrix.

Inter-reef connectivity—the proportion of larvae spawned from a reef that successfully settled in any non-natal reef—was calculated by summing each row of the connectivity matrix excluding local retention.

Metapopulation model structure

We modified a size-structured, discrete-time matrix metapopulation model originally developed by Puckett and Eggleston (2016) of the form,

$$n(t+1) = \mathbf{A}n(t)$$

where n is a vector containing the number of individuals in each size class at time t and $\mathbf{A}$ is a metapopulation projection matrix that represents demographic transitions and per capita fecundity (Caswell 2001). We divided n on the basis of size classes where elements in vector n contained the abundance of oysters in one of three size classes: 0–30 mm (recruits), 30–75 mm (subadults), and 75+ mm (adults, harvestable size).

The model time step was divided into three intra-annual seasonal periods corresponding to demographic sampling (see *Estimating demographic rates via field sampling* above) and oyster biology (Puckett and Eggleston 2016). The projection matrix, $\mathbf{A}$, was parameterized separately for each season: $\mathbf{A}^{\text{spring}}$—1 May to 30 June corresponding to peak oyster fecundity, $\mathbf{A}^{\text{summer}}$—1 July to 31 August corresponding to secondary peaks in oyster fecundity, and $\mathbf{A}^{\text{fall/winter}}$—1 September to 30 April corresponding to no fecundity. Growth and survival also differed in each seasonal projection matrix (see description of transition probabilities below). Projection matrices did not vary inter-annually as reef type-specific demographic data were pooled to ensure sufficient sample sizes for estimating demographic parameters in $\mathbf{A}^x$ (McMurray et al. 2010, Puckett and Eggleston 2016).

Seasonal metapopulation projection matrices were parameterized separately for each k reef ($\mathbf{A}_k^x$) and decomposed into the sum of two matrices, $\mathbf{T}_k^x$ and $\mathbf{F}_k^x$, where $\mathbf{T}_k^x$ describes transition probabilities in reef k during season x and $\mathbf{F}_k^x$ describes per capita fecundity in reef k during season x. The diagonal elements of $\mathbf{T}_k^x$ describe the probability of individuals in reef k and size class i surviving and remaining in size class i (i.e., stasis; $P_{i,k}$; Fig. 2), and the subdiagonal elements describe the probability of surviving and
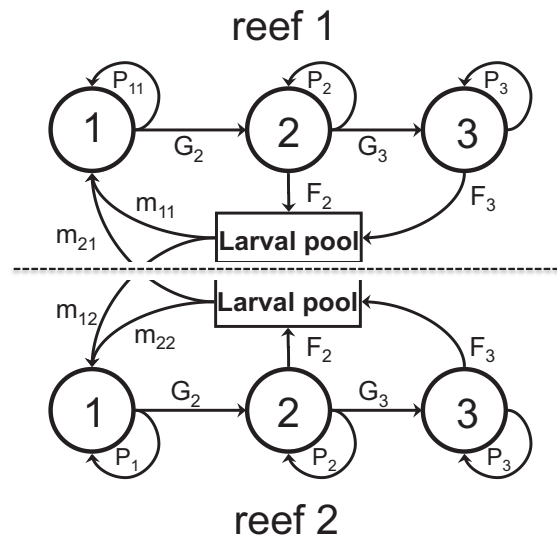

Fig. 2. A simplified life cycle graph (adapted from Puckett and Eggleston 2016) depicting the spatially explicit, size-structured matrix metapopulation model used in this study. Two subpopulations (separated by dotted line) and three size classes (circles) are shown. The model used in the present study consisted of 646 reefs and three size classes. Model parameters are as follows: P_i is the probability of surviving and remaining in size class i; G_j is the probability of surviving and growing into size class j; F_i is the per capita fecundity of size class i; and m_{jk} is the proportion of larvae spawned in reef j that settle in reef k.

growing into size class j ($G_{i,k}$). Reef type- and season-specific growth and survival transition probabilities were estimated using the methods described in *Estimating growth and survival transition probabilities* above. Elements along the first row of $\mathbf{F}_k^x$, the only nonzero values in $\mathbf{F}$, describe per capita fecundity of individuals in reef k and size class i ($F_{i,k}$). Elements of $\mathbf{F}_k^x$ were adjusted for density-dependent fertilization success based on Levitan (1991) as follows:

$$\% \text{ fertilization} = 0.49 \times D^{0.72}$$

where D is total oyster density per m^2. Fertilization success was capped at 100% in the event oyster densities were sufficiently high to generate fertilization success >100%. The larvae spawned from reef j were calculated as the product of a reef's per capita fecundity matrix ($\mathbf{F}_j^x$) and $n_{j(t)}$. Larvae were distributed among reefs based on elements of the connectivity matrix, $\mathbf{M}$,

at time t. Elements of $\mathbf{M}$ describe the proportion of larvae released from reef j that survive to settle in reef j ($m_{j,k}$; Fig. 2). Connectivity pathways included both local retention and inter-reef connectivity. Settlement occurred at the midpoint of the model time step (i.e., $t + 0.5$) and new settlers in reef j survived to time $t + 1$ with probability $P^*_{1,j}$ adjusted for half a time step (Caswell 2001, Puckett and Eggleston 2016).

The complete metapopulation model, adapted from Puckett and Eggleston's (2016) original model, was expressed as:

$$N(t+1) = \sum \begin{pmatrix} n_{1(t+1)} \\ \vdots \\ \overline{n_{646(t+1)}} \end{pmatrix} = \left(\begin{bmatrix} T_{1^x} & \cdots & 0 \\ \vdots & \ddots & \vdots \\ 0 & \cdots & T_{646^x} \end{bmatrix} + \begin{bmatrix} P^*_{1,1}\left(m_{1,1}\mathbf{F}^x_1\right) & \cdots & P^*_{1,646}\left(m_{646,1}\mathbf{F}^x_{646}\right) \\ \vdots & \ddots & \vdots \\ P^*_{1,646}\left(m_{1,646}\mathbf{F}^x_1\right) & \cdots & P^*_{1,646}\left(m_{646,646}\mathbf{F}^x_{646}\right) \end{bmatrix} \right) \begin{pmatrix} n_{1(t)} \\ \vdots \\ \overline{n_{646(t)}} \end{pmatrix}$$

where N is metapopulation size at time t, $n_{k(t)}$ is a subvector containing the abundance of oysters in each size class in reef k at time t, $\mathbf{T}^x_k$ is a submatrix representing the transition probabilities of each size class in reef k at time t during season x, $\mathbf{F}^x_k$ is a submatrix representing the per capita fecundity of each size class in reef k at time t during season x, and $m_{j,k}$ and $P^*_{1,j}$ are defined as above (Lewis et al. 1997, Caswell 2001, Puckett and Eggleston 2016). Population vectors at each reef, n_k, were seeded with reef-specific empirical estimates (or interpolated for reefs not sampled) of an initial population size based on oyster density and size structure scaled to reef area (Table 1, see *Estimating demographic rates via field sampling* above). Metapopulation abundance was projected over a five-year period from May 2012 to April 2017.

Quantifying metapopulation and source–sink dynamics

Overall metapopulation growth rate was calculated as follows:

$$\lambda_M(t) = \sum_{j=1}^{646} \lambda_{C,j}(t) \left(\frac{n_{j(t)}}{N(t)} \right)$$

where ($\lambda_{C,j}(t)$) is reef j's contribution to the metapopulation at time t (Figuiera and Crowder

2006, Puckett and Eggleston 2016) and $N(t)$ and $n_{j(t)}$ are defined above. Values of $\lambda_M(t) \geq 1$ indicate a persistent or expanding metapopulation during time t, whereas $\lambda_M(t) < 1$ indicates a contracting metapopulation during time t. We generated a time-series plot to depict λ_M across the five-year model time frame.

Each reef's contribution to the metapopulation (i.e., subpopulation status as a net source or sink) was calculated based on Figuiera and Crowder (2006) as follows:

$$\lambda_{C,j}(t) = \left[\mathbf{T}^x_j n_{j(t)} \right] + \left[\sum_{j=1}^{646} P^*_{1,k}\left(m_{jk}\mathbf{F}^x_j n_{j(t)} \right) \right]$$

where variables are defined as above and $\lambda_{C,j}(t) \geq 1$ indicates reef j functioned as a source during time t and $\lambda_{C,j}(t) < 1$ indicates reef j functioned as a sink during time t. By calculating reef source–sink status in this manner, reefs are credited with births to any reef within the metapopulation (including itself) and penalized for deaths that occur within the reef. By this definition, a source contributes positively to metapopulation persistence regardless of whether local retention is sufficient for self-persistence.

Metapopulation and source–sink dynamics were evaluated under three distinct proportional daily larval mortality rates: 7.5%, 10%, and 20% d^{-1}, based on literature-derived relationships between larval duration and mortality (Mann and Evans 1998). As further described below in *Results*, each larval mortality scenario yielded widely varying metapopulation and source–sink dynamic outcomes. We describe each scenario and provide detailed descriptions of the 10% proportional daily larval mortality scenario that was chosen for more detailed simulations based on agreement of the model output with prior field-based observations.

Evaluating reef type- and size class-specific population trajectories.—Time-series plots were generated to depict reef type- and size class-specific population trajectories. Specifically, the mean per reef population size associated with a given reef type and size class was plotted across the five-year model time frame.

Evaluating spatiotemporal variation in source–sink structure.—Box and whisker plots were generated to depict season (i.e., May–June vs. July–August) and reef type-specific source–sink status (i.e., λ_c),

and a map depicted the frequency of $\lambda_c \geq 1$ at all reefs across the five-year model time frame was produced.

Estimating the degree and relative importance of local larval retention vs. inter-reef connectivity.—The degree and relative importance of local larval retention and inter-reef connectivity for a given reef type were based on the average percent of larvae (i.e., across all 10 simulated dispersal events) retained locally vs. exported between reefs. Local larval retention includes all larvae originating from a given reef that settle on the same reef. Larval export includes all larvae originating from a given reef that settle on a different reef. For those reefs exhibiting $\lambda_c \geq 1$, the average percent of larvae retained locally vs. exported between reefs for each level of frequency of $\lambda_c \geq 1$ (i.e., 10–50% of the 10 simulated dispersal events) was evaluated to determine possible larval connectivity-derived drivers of reefs identified as frequent population sources.

Assessing validity of model output.—Observed vs. model predicted population sizes were compared to quantitatively assess validity of model output (Fig. 3). Specifically, estimates of observed population size derived from field sampling of subtidal natural and cultch reefs in August 2012 (Peters et al. 2017), as well as subtidal sanctuary reefs in August 2012 and 2013, and October 2014 (North Carolina Division of Marine Fisheries, unpublished data), were compared with estimates of predicted population size derived from metapopulation simulations corresponding to the same time period in the present study. Because oyster density estimates derived from field samplings at different time points (i.e., 2006–2008 for subtidal sanctuary reefs and 2014–2015 for intertidal natural and hardened shoreline reefs) were used to parameterize the model, and the model time step was initialized to May 2012, the above-stated field-derived data represented the only available data for valid comparison.

RESULTS

Areal footprint, density, and population estimates by reef type

In terms of areal footprint, subtidal natural oyster reefs are the predominant reef type within the APES, with an estimated 301 unique reefs encompassing an estimated total reef area of 934.27 ha
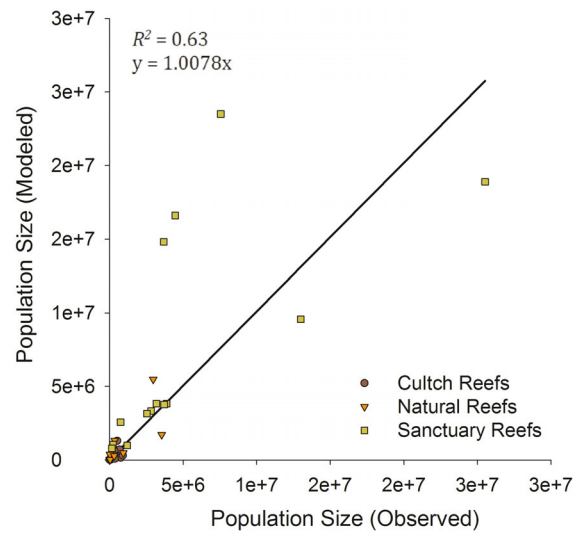

Fig. 3. Relationship between observed and predicted population sizes at subtidal cultch (red circles), subtidal natural (orange triangles), and subtidal sanctuary reefs (yellow squares). Estimates of observed population size are derived from field sampling of natural subtidal and cultch reefs in August 2012 and sanctuaries in August 2012 and 2013, and October 2014. Estimates of predicted population size are derived from metapopulation model simulations corresponding to the same time period in the present study (under the 10% larval mortality d^{-1} scenario). Solid line is the best fitting linear regression, forced through the origin.

(89.8% of total reef area; Table 1, Fig. 1). Subtidal sanctuary reefs were the next largest reef type, with the boundaries of these 14 reefs encompassing a total reef area of 66.02 ha (6.3% of total reef area). Subtidal cultch reefs were the third largest reef type by total reef area, with an estimated 53 reefs encompassing 15.32 ha (1.5% of total reef area). Intertidal natural reefs in Pamlico and Core Sounds occupied similar total reef areas, with 59 intertidal natural reefs occupying 10.43 ha (1.0% of total reef area) in Pamlico Sound, and 72 intertidal natural reefs occupying 11.82 ha (1.1% of total reef area) in Core Sound. Hardened shoreline reefs occupied the smallest total reef area, with 149 hardened shorelines encompassing 2.69 ha (0.26% of total reef area).

Average initial population densities were highest on intertidal natural reefs in Core Sound, followed closely by subtidal sanctuary reefs

(842 oysters m^{-2} and 670, respectively; Table 1). Conversely, subtidal cultch reefs and intertidal natural reefs in Pamlico Sound harbored moderate population densities (152 oysters m^{-2} and 121, respectively), whereas hardened shoreline reefs and subtidal natural reefs harbored the lowest population densities (69 oysters m^{-2} and 61, respectively). When initial density was scaled by reef area to estimate the initial population size of individual reefs used to seed the metapopulation model (see *Estimating demographic rates via field sampling* above), the average initial population size of subtidal sanctuary reefs was approximately one order of magnitude greater than the next highest reef types, which were subtidal natural reefs and intertidal natural reefs in Core Sound (Table 1). Subtidal cultch reefs and intertidal natural reefs in Pamlico Sound contained similar initial population sizes (average of ~400,000 individuals). Hardened shoreline reefs contained the smallest initial population sizes (average of ~70,000 individuals; Table 1).

The average initial size structure of subtidal natural reefs and subtidal cultch reefs was comparable, with ~one-half of the population contained within the subadult size class, ~one-third of the population within the recruit size class, and ~one-sixth of the population within the adult size class (Table 1). Intertidal natural reefs in Pamlico and Core Sounds contained similar average size structures to subtidal natural and cultch reefs, with slightly greater populations of subadults and recruits and less than one-tenth of the population within the adult size class. Average initial size structure of subtidal sanctuary reefs contained ~one-quarter of the population within the recruit size class, ~two-thirds of the population within the subadult size class, and less than one-tenth of the population within the adult size class. Hardened shoreline reefs contained an average initial size structure with ~two-thirds of the population within the subadult size class, ~one-third within the adult size class, and less than one-twentieth of the population within the recruit size class.

Larval connectivity

Variability in the dominant wind direction during the two primary spawning periods for oysters in Pamlico Sound (i.e., May–June and July–August 2012–2016) yielded widely varying larval dispersal patterns. We used a residual sums of square (RSS) analysis of average frequencies for wind speed and direction (i.e., across 5 m s^{-1} speed bins and 10° directional bins; sensu Puckett et al. 2014) to determine times of average wind conditions when the RSS was lowest, and highest RSS to determine anomalous wind conditions. Based on this analysis, winds within the APES were predominately southwesterly (toward northeast) at mean speeds of 4–5 m s^{-1}. Average wind conditions from 2012 to 2016 were best represented by July–August 2013, and larval dispersal patterns during this time largely reflected northeast transport of larvae (Fig. 4). The period of May–June 2012 represented anomalously strong and variable northeasterly winds (toward southwest), with dispersal patterns displaying highly variable directionality of larval connections between natal and settled reefs (Fig. 5). The period July–August 2012 represented the strongest and most frequent southwesterly winds (toward northeast), and dispersal patterns reflected strong larval transport from southern natal reefs in the APES toward northeastern reefs (Fig. 6). Additional figures depicting larval connectivity during the other dispersal periods are included in the Supporting Information (Appendix S1: Figs. S2–S8).

Larvae were more frequently exported to different reefs than they were retained locally (Table 4). On average, ~0.4% of larvae were retained locally (i.e., all larvae originating from a given reef that settle on the same reef), whereas ~18% of larvae were exported (i.e., all larvae originating from a given reef that settle on a different reef). Natural subtidal reefs exported the greatest percentage of larvae to other reefs (~26%), followed by subtidal cultch and sanctuary reefs. Hardened shorelines and natural intertidal reefs in Pamlico Sound exported similar amounts of larvae and retained very few locally. Natural intertidal reefs in Core Sound exported the lowest percentage of larvae to other reefs (~5%).

Metapopulation status and source–sink dynamics

Variation in proportional daily larval mortality rates between 7.5%, 10%, and 20% d^{-1} yielded widely varying outcomes for total metapopulation abundance (Appendix S1: Fig. S9). The 7.5% d^{-1} larval mortality rate yielded a rapidly growing metapopulation (Appendix S1: Fig. S9a),
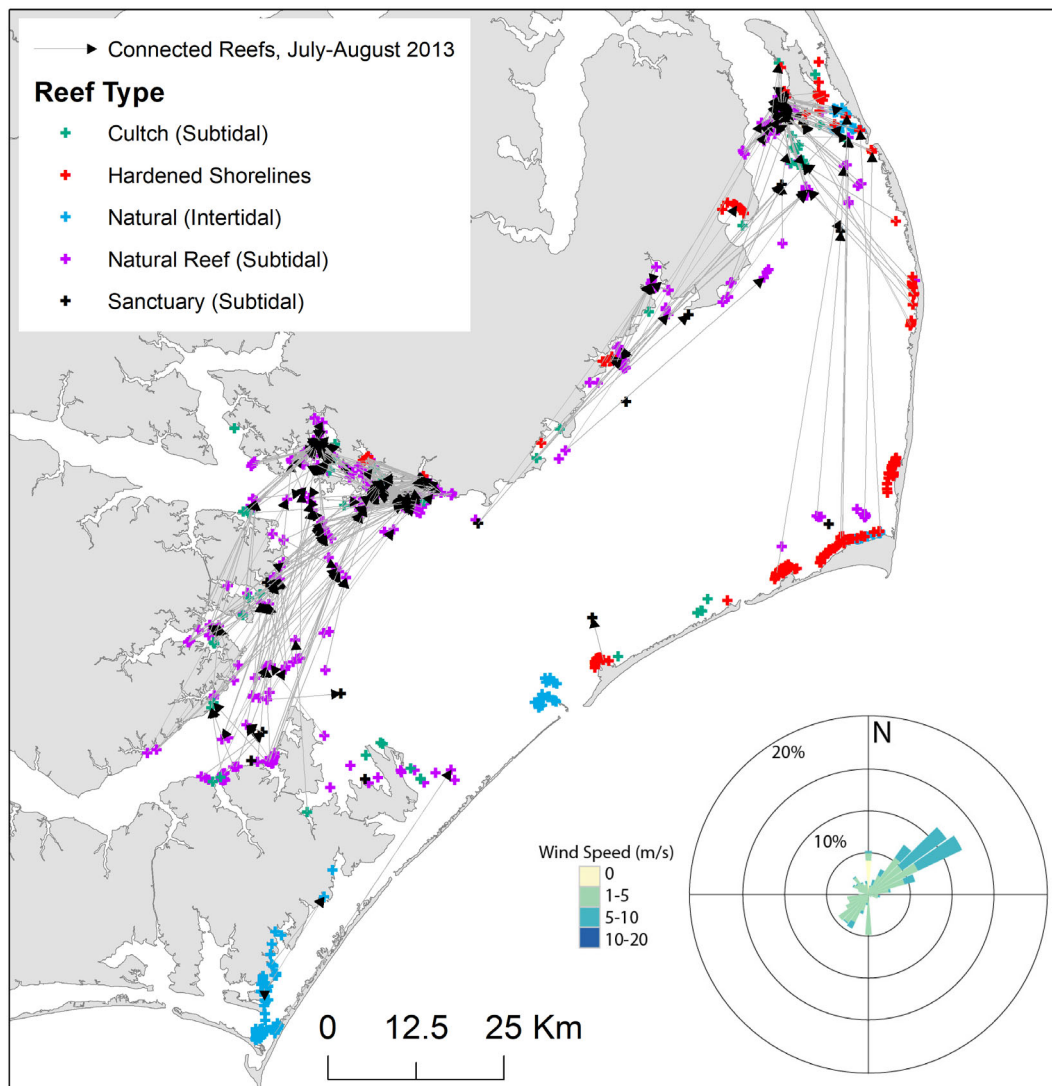
Fig. 4. Map depicting larval dispersal patterns during a period of average wind conditions (i.e., predominantly southwesterly winds, toward northeast) during July–August 2013. Lines depict connections between natal and settled reef locations (arrowheads point toward settled reef locations). Note that lines depict the least-cost path between reefs and not the actual dispersal path, and only a random subset (5%) of all connections are shown for illustrative purposes.

the 10% d^{-1} larval mortality rate yielded a generally stable, but slightly declining metapopulation (Appendix S1: Fig. S9b), whereas the 20% d^{-1} larval mortality rate yielded a rapidly declining metapopulation (Appendix S1: Fig. S9c). As the 10% d^{-1} larval mortality rate yielded overall metapopulation trends that most closely aligned with field-based observations (e.g., episodic recruitment on hardened shorelines, Theuerkauf et al.

2017; Fig. 3), we present figures depicting reef type- and size class-specific population trajectories by applying a 10% d^{-1} larval mortality rate (Fig. 7). Population trajectories and metapopulation summary statistics applying 7.5% and 20% d^{-1} larval mortality rates are provided in the Supporting Information (Appendix S1: Figs. S10–S23).

Overall oyster population trends by reef type showed an overall slight decline across reef types
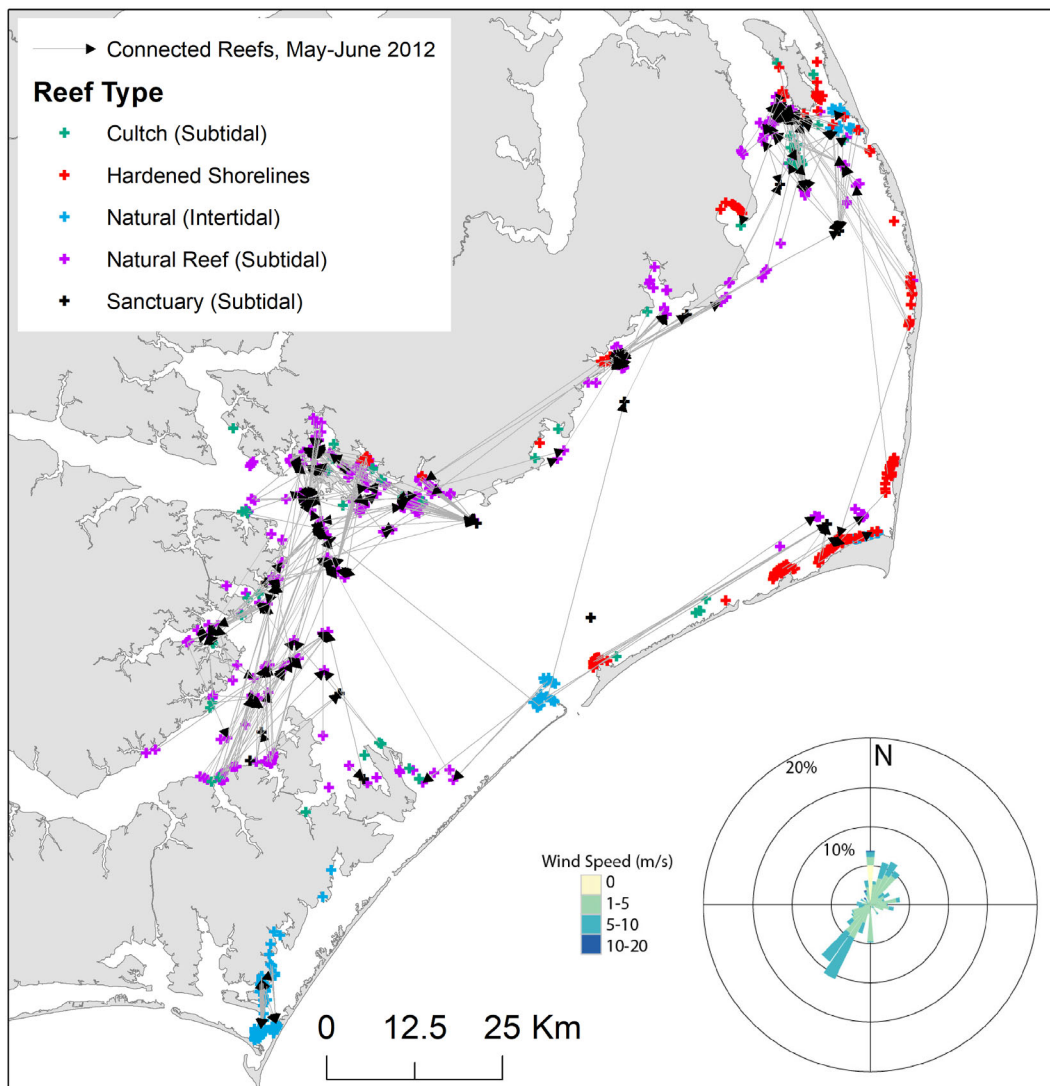
Fig. 5. Map depicting larval dispersal patterns during a period of anomalously strong northeasterly winds (toward southwest) during May–June 2012. Lines depict connections between natal and settled reef locations (arrowheads point toward settled reef locations). Note that lines depict the least-cost path between reefs and not the actual dispersal path, and only a random subset (5%) of all connections are shown for illustrative purposes.

(Fig. 7; Appendix S1: Fig. S24); however, spatiotemporal variation in recruitment yielded substantial differences in population trajectories (Fig. 7; Appendix S1: Fig. S25). For example, the population trajectory for subtidal natural and cultch reefs (Fig. 7A,B; Appendix S1: Fig. S25) was oscillatory in response to consistently high recruitment, but was generally stable across time around a mean population size. In contrast, the population trajectory for hardened shorelines

and intertidal natural reefs in Pamlico Sound (Fig. 7D,E; Appendix S1: Fig. S25) showed an overall decline with punctuated increases in response to episodic recruitment. Spatiotemporal variation in recruitment patterns was generally manifested in subadult and adult size classes in subsequent time steps (Fig. 7; Appendix S1: Figs. S26, S27). For example, substantial recruitment on hardened shorelines during the May–June recruitment event of 2014 (Fig. 7D;
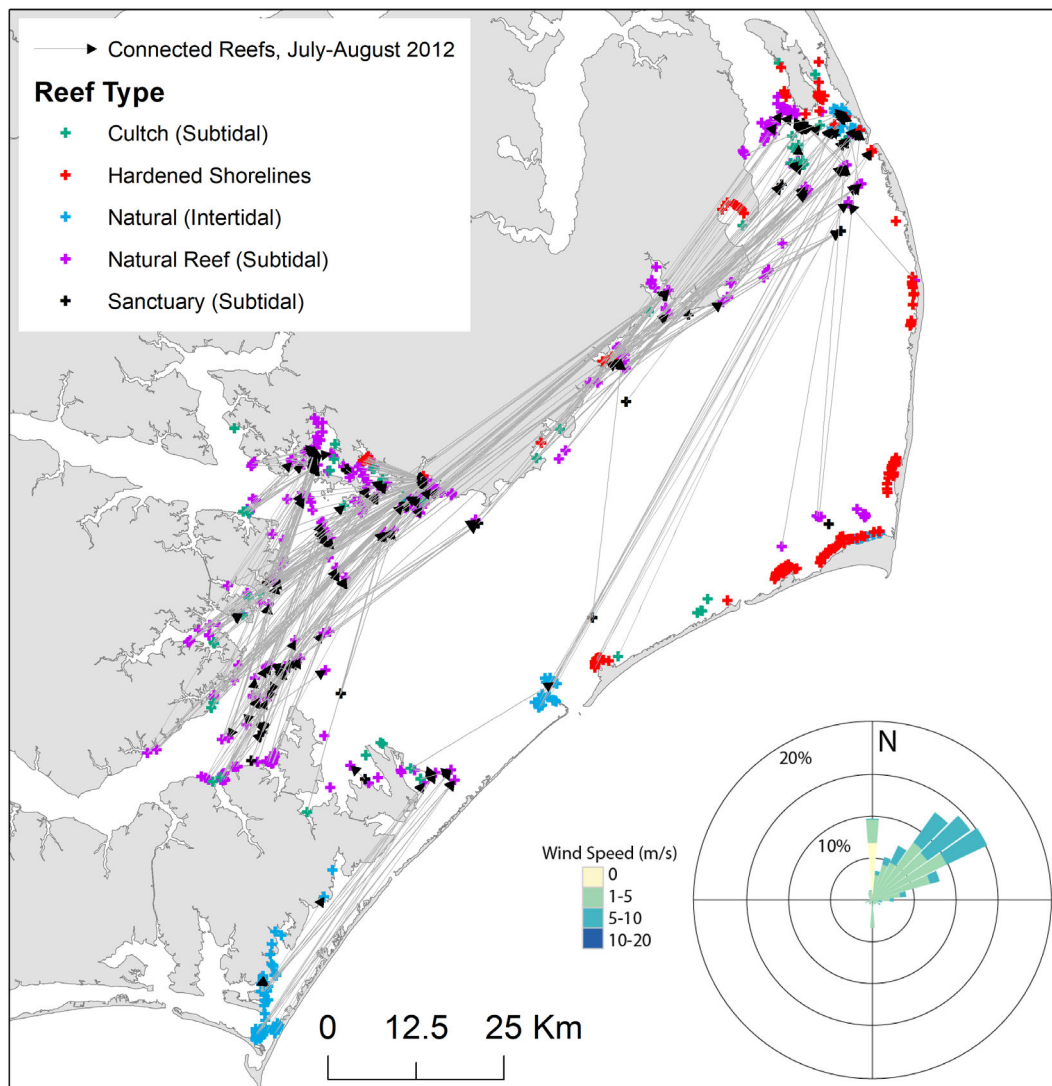
Fig. 6. Map depicting larval dispersal patterns during a period of anomalously strong southwesterly winds (toward northeast) during July–August 2012. Lines depict connections between natal and settled reef locations (arrowheads point toward settled reef locations). Note that lines depict the least-cost path between reefs and not the actual dispersal path, and only a random subset (5%) of all connections are shown for illustrative purposes.

Appendix S1: Fig. S25) yielded increases in subadult (Appendix S1: Fig. S26) and adult (Appendix S1: Fig. S27) populations on hardened shorelines in the subsequent time steps. In contrast, periods of low recruitment yielded decreases in subadult and adult populations. For example, low levels of recruitment on hardened shorelines in 2015 (Fig. 7D; Appendix S1: Fig. S25) yielded declining subadult (Fig. 7D; Appendix S1: Fig. S26) and adult (Fig. 7D; Appendix S1: Fig. S27) populations. The exception to this pattern occurred on subtidal sanctuaries where subadult (Fig. 7C; Appendix S1: Fig. S26) and adult (Fig. 7C; Appendix S1: Fig. S27) dynamics were not as oscillatory in response to variation in recruitment patterns (Fig. 7C; Appendix S1: Fig. S25). Overall metapopulation growth rate (λ_M) exceeded 1 during all model time steps corresponding to the peak primary spawning event (May–June), but

Table 4. Average percent of larvae (i.e., across all 10 simulated dispersal events) retained locally vs. exported between reefs.

Reef type	Local retention (%)	Larval export (%)
Overall	0.38	17.66
Natural (subtidal)	0.64	26.03
Cultch (subtidal)	0.10	23.77
Sanctuary (subtidal)	0.71	19.76
Hardened shorelines	0.06	8.35
Natural (intertidal, Core Sound)	0.41	5.33
Natural (intertidal, Pamlico Sound)	0.01	7.17

Notes: Local larval retention includes all larvae originating from a given reef that settle on the same reef. Larval export includes all larvae originating from a given reef that settle on a different reef.

was less than 1 during all other model time steps (i.e., indicative of a nonpersistent metapopulation; Appendix S1: Fig. S28).

Source–sink status (λ_c) of reefs varied widely by reef type and between the May–June and July–August spawning peaks for oysters in Pamlico Sound (Fig. 8; Appendix S1: Fig. S29). During primary spawning and recruitment periods in May–June, subtidal sanctuaries were the only reef type with a mean λ_c exceeding 1, indicating many sanctuaries served as metapopulation sources (Fig. 8). Some subtidal natural and cultch reefs served as sources, whereas fewer intertidal natural reefs in Pamlico and Core Sounds served as sources. No hardened shorelines functioned as sources during the May–June time steps. During secondary spawning and recruitment periods in July–August, only a small portion of subtidal sanctuaries, intertidal natural reefs in Core Sound, and hardened shorelines functioned as episodic sources (Table 5; Appendix S1: Fig. S29).

Reefs serving as frequent sources to the metapopulation (i.e., high frequency of $\lambda_c > 1$ across model time steps) were generally located in the northeastern portion of Pamlico Sound (Fig. 9). Other frequent sources were distributed widely throughout Pamlico Sound, often in central locations within the sound and not within embayments. Subtidal sanctuaries were the most frequent sources to the metapopulation (Table 5), followed by natural subtidal reefs and subtidal cultch reefs. Natural intertidal reefs and hardened shorelines were occasional sources. Of the

reefs that served as frequent sources, local larval retention was generally greater than average (e.g., ~2% and ~3% vs. ~0.5%) and larval export was also generally greater than average (>22% vs. ~18%).

Discussion

We integrated demographic rates and dispersal to simulate dynamics of an entire oyster metapopulation. Using this modeling framework, we answered three broad questions, each with important implications for conservation and management. (1) What is the relative importance of no-harvest sanctuary oyster reefs to the overall metapopulation? Sanctuaries served as the most frequent subpopulation sources, contributing disproportionately to the metapopulation relative to their reef footprint. Representing only 6.2% of the total reef area, sanctuaries harbored 19% (±2) of all oysters and produced 25% (±6) of all larvae that settled within the metapopulation. In contrast, subtidal natural reefs, the predominant reef type and open to harvest, accounted for 90% of total reef area, yet harbored only 70% (±2) of all oysters and produced 68% (±8) of all larvae that settled within the metapopulation. (2) Is there consistency in source–sink structure in space and time that could inform conservation and management? Source–sink status of reefs varied widely in space and time, although some generalities emerged. Reefs serving as frequent sources were generally located in the northeastern portion of the study system where hydrodynamics enhanced larval connectivity. Interestingly, given their highly degraded state and poor demographics, natural subtidal reefs were the second most frequent sources among all reef types. Management to restore and/or protect from harvest these source subtidal natural reefs may promote metapopulation persistence. (3) Are metapopulation dynamics driven more by inter-reef larval export or local larval retention processes and associated subpopulation (i.e., reef) demographic rates? Rates of inter-reef larval connectivity far exceeded rates of local retention, suggesting that larval connectivity is likely a more important driver of metapopulation dynamics than subpopulation demographics within this system (Figueira 2009). Restoration of new subtidal cultch reefs or

establishment of additional sanctuaries should explicitly consider larval connectivity in their design.

This study provides five major insights that build on and extend previous findings regarding marine metapopulations. First, the rates and extent of population connectivity via larval dispersal have previously been identified as crucial in determining whether metapopulation structure actually exists (Kritzer and Sale 2006). Within the present study, the network of oyster reef subpopulations was found to be buffered and subsidized through larval dispersal, which is consistent with the notion of an asynchronous oyster metapopulation in space and time. Second, the challenge in specifying causes of recruitment variation within a metapopulation is generally due to the inability to specify either the spatial scale over which subpopulations are interconnected, or the extent of recruitment subsidies to each subpopulation due to contributions from other sources (Kritzer and Sale 2006). The spatial domain in the present study encompassed all known potential sources of oyster larvae within the estuarine metapopulation (646 reefs; area of ~7800 km^2), and larval connectivity matrices were generated that characterized the frequency of local retention vs. larval subsidy among subpopulations (i.e., ~0.5% vs. ~18%). Third, there are very few examples of metapopulation studies in which the relative importance of within-patch demographic rates vs. larval connectivity to metapopulation dynamics is demonstrated (Figueira 2009, Puckett and Eggleston 2016, Castorani et al. 2017 and references therein). For example, Figueira (2009) evaluated the relative importance of connectivity vs. subpopulation-scale demography by applying a spatially explicit, age-structured simulation model to a coral reef fish (damselfish, *Stegastes partitus*) metapopulation in the Florida Keys, USA (Crowder and Figueira 2006, Figueira et al. 2008). Elasticity analyses in Figueira (2009) indicated that patch-scale (i.e., subpopulation) contributions as a source or sink were more sensitive to demographic parameters (particularly survival) than larval connectivity. Castorani et al. (2017) quantified metapopulation connectivity of a marine foundation species (giant kelp, *Macrocystis pyrifera*) across 11 yr and approximately 900 km of coastline in California, USA, by estimating population fecundity with satellite imagery and propagule dispersal using a high-resolution ocean circulation model. They varied the temporal complexity of different connectivity measures and determined that fluctuations in population fecundity, rather than fluctuations in dispersal, were the dominant driver of variation in connectivity and metapopulation recovery and persistence. In the present study, the overall pattern of oyster metapopulation decline with slight recovery following the spawning peak of oysters in May–June suggests that larval connectivity, in combination with relatively high fecundity in no-take sanctuaries during the initial spawning peak of oysters, appears more important than patch-scale demographic rates such as growth and survival to metapopulation dynamics. The previous and related studies (e.g., Aiken and Navarrete 2011, Carroll et al. 2020) highlight the importance of considering both larval connectivity and subpopulation demographic variability when characterizing metapopulation and source–sink dynamics. Fourth, spatiotemporal variation in hydrodynamics (Watson et al. 2012), environmental variables (Aiken and Navarrete 2011), and subpopulation demographic rates (Figueira 2009) can drive variation in source–sink structure. An important contribution of the present study is the characterization of both variation and relative consistency in source–sink structure of the oyster metapopulation in Pamlico Sound, North Carolina, USA. Information on consistency in source–sink structure in marine metapopulations is scarce, yet is important to guiding management, conservation, and restoration efforts. Lastly, climate change, species range shifts, and human impacts such as overfishing and habitat alteration will likely alter larval connectivity and subpopulation demographics of many marine species. The empirically grounded, metapopulation modeling approach used in this study can be applied to conservation and restoration efforts optimized to future scenarios, such as the recent application in California, USA, to evaluate the impact of reserve network design on the resiliency of fisheries to the effects of climate change (Rassweiler et al. 2020).

Oyster metapopulation and source–sink dynamics

Overall metapopulation trends.—The 10% d^{-1} larval mortality rate yielded an overall stable, yet slightly declining metapopulation (Fig. 7G). Increases in overall metapopulation abundance

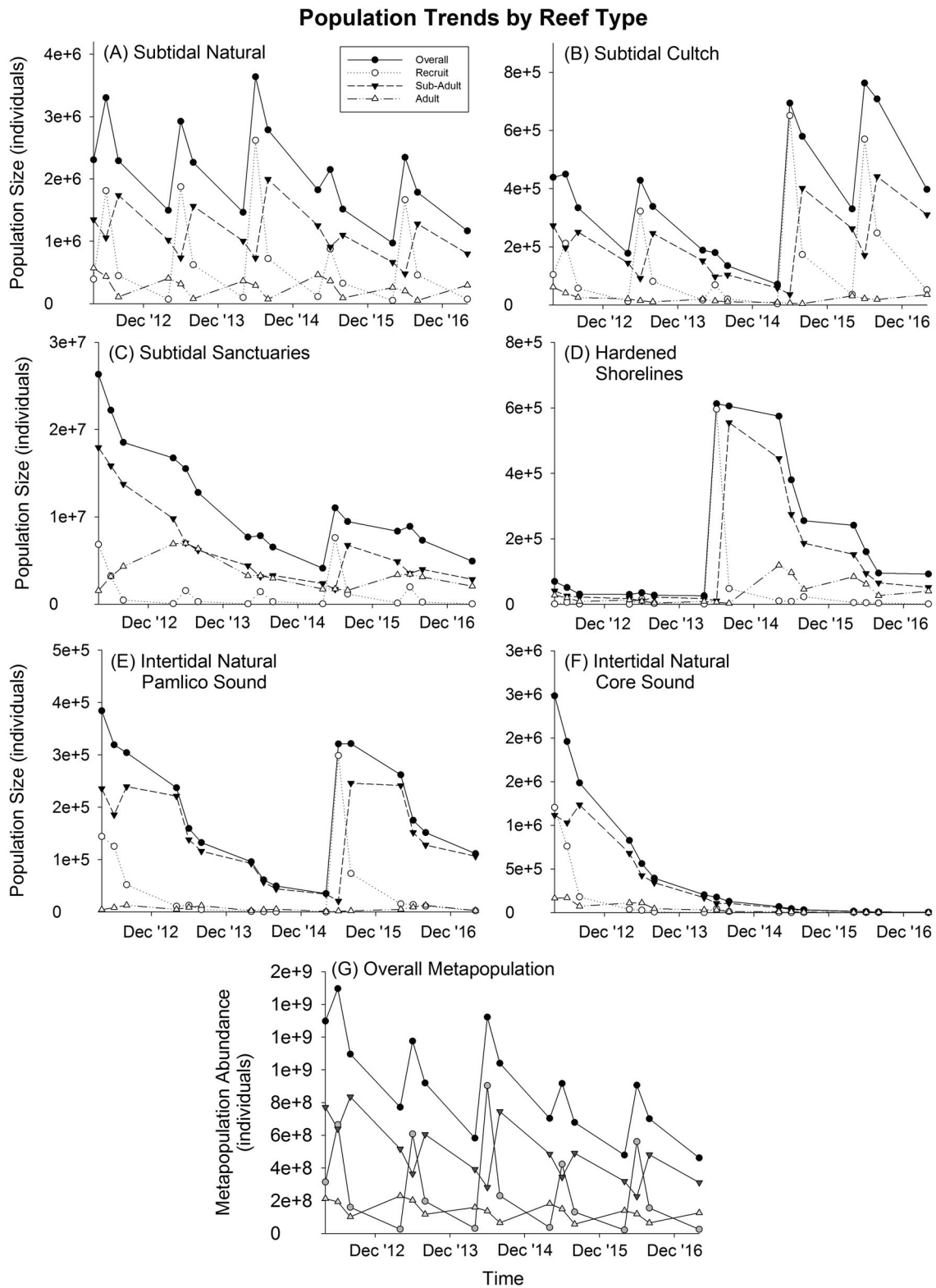**Population Trends by Reef Type**

Fig. 7. Population trends by reef type and size class (A–F), including overall metapopulation trends (G), across

(Fig. 7. *Continued*)
the five-year model time frame under the 10% larval mortality d^{-1} scenario. Points represent the average population size on a given reef type by size class (A–F), and the overall metapopulation size by size class (G), at a given time step.
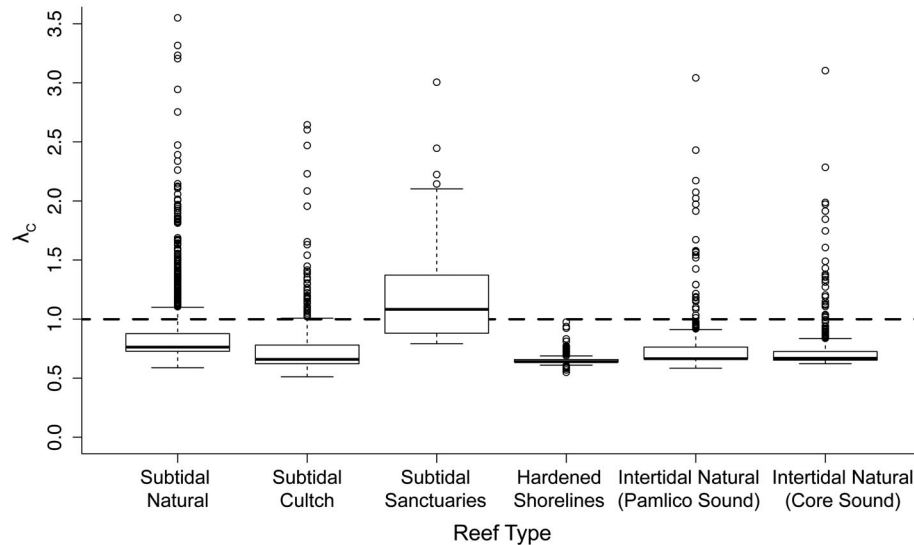

Fig. 8. Source–sink status (λ_c) of each reef (by reef type) during each May–June time step between 2012 and 2016 under the 10% larval mortality d^{-1} scenario. $\lambda_c \geq 1$ indicates a given reef functioned as a source during time t, and $\lambda_c < 1$ indicates a given reef functioned as a sink during time t.

corresponded with the period following the primary spawning peak (i.e., May–June) within the system. Increases in recruit abundance after the spawning peak were followed in subsequent periods with increases in subadult and adult abundance corresponding with survival and growth of individuals into the next size class. The overall pattern of metapopulation decline with slight recovery following the spawning peak (Appendix S1: Fig. S9b) is indicative of the importance of recruitment within the system—a finding consistent with previous studies (e.g., Caley et al. 1996). The patterns of the overall metapopulation growth rate (λ_M) provide further support for this notion (Appendix S1: Fig. S28), wherein λ_M exceeds 1 and the metapopulation size increases only in the period following the primary spawning peak. These findings, wherein a network of oyster reef subpopulations was buffered and subsidized through larval dispersal, lend strong support to the notion of a spatial and temporal, asynchronous oyster metapopulation within the APES (sensu Levins 1969).

Subpopulation trajectories.—Overall oyster subpopulation trends by reef type exhibited an overall slight decline across reef type (Fig. 7), and spatiotemporal variation in recruitment generally impacted population trajectories. Subtidal natural and cultch reefs generally received consistent recruitment during the annual primary and secondary spawning peaks (Fig. 7A,B; Appendix S1: Fig. S25). Other reef types, such as hardened shorelines and intertidal natural reefs in Pamlico Sound (Fig. 7D,E; Appendix S1: Fig. S25), received episodic recruitment—a finding consistent with a field-based study that examined oyster density and demographic rates on hardened shorelines and intertidal natural reefs in Pamlico Sound (Theuerkauf et al. 2017). The spatial distribution of reef types yielded a substantial influence on

Table 5. Total number of reefs of a specific reef type associated with a $\lambda_c > 1$ (i.e., $\lambda_c \geq 1$ indicates a given reef functioned as a source during time t) at varying frequencies.

Frequency of $\lambda_c > 1$ (%)	Local retention (%)	Larval export (%)	Reef type
50	1.51	24.36	One natural subtidal reefs, three sanctuaries
40	2.50	24.89	Seven natural subtidal reefs, four sanctuaries
30	0.24	27.61	25 natural subtidal reefs, four cultch reefs, four sanctuaries, two hardened shorelines
20	1.36	26.87	29 natural subtidal reefs, five cultch reefs, one sanctuary, three natural intertidal reefs (Core Sound), five hardened shorelines
10	0.38	22.05	53 natural subtidal reefs, 17 cultch reefs, four natural intertidal reefs (Pamlico Sound), 22 natural intertidal reefs (Core Sound), 16 hardened shorelines
All	**0.70**	**24.21**	**115 natural subtidal reefs (38%), 12 sanctuaries (86%), 26 cultch reefs (49%), 23 hardened shorelines (15%), 25 natural intertidal reefs (Core Sound; 35%), four natural intertidal reefs (Pamlico Sound; 7%)**

Notes: For each level of frequency of $\lambda_c \geq 1$, the corresponding average percent of larvae retained locally vs. exported between reefs is provided. Local larval retention includes all larvae originating from a given reef that settle on the same reef. Larval export includes all larvae originating from a given reef that settle on a different reef.

recruitment patterns. For example, subtidal natural and cultch reefs, which are distributed consistently throughout the APES, generally receive regular recruitment (Fig. 7A,B; Appendix S1: Fig. S25). Conversely, hardened shorelines, which are concentrated primarily along the eastern shore of Pamlico Sound, received substantial, episodic recruitment following the May–June 2014 spawning event (Fig. 7D; Appendix S1: Fig. S25), which corresponded with a period of strong southwesterly winds (Appendix S1: Fig. S3). Observed spatiotemporal variation in recruitment patterns generally led to similar subsequent patterns in subadult and adult size classes (Fig. 7; Appendix S1: Figs. S26, S27).

Variation in oyster demographics (i.e., growth and survival transition probabilities; Table 2) also yielded varied subpopulation-level outcomes by reef type. For example, while subtidal natural reefs exhibited substantial, oscillatory population booms and busts (Fig. 7A; Appendix S1: Fig. S27), the improved demographics (i.e., growth and survival transition probabilities) associated with subtidal sanctuaries (Fig. 7C; Appendix S1: Fig. S27) yielded subpopulations less directly impacted by recruitment variation. The less oscillatory subadult (Fig. 7C; Appendix S1: Fig. S26) and adult (Fig. 7C; Appendix S1: Fig. S27) subpopulations on subtidal sanctuaries in response to variation in recruitment patterns (Fig. 7C; Appendix S1: Fig. S25) provide

evidence of the buffering capacity of no-take, sanctuary subpopulations and an ability to withstand periods of reduced recruitment. This finding is consistent with field-based observations of these protected reefs within the system (Puckett and Eggleston 2012).

Spatiotemporal variation in oyster source-sink dynamics.—Source–sink status (λ_c) of reefs varied widely by reef type and between the May–June and July–August spawning peaks in the APES (Fig. 8; Appendix S1: Fig. S29). During the primary spawning event (May–June), subtidal sanctuaries were the only reef type with a mean λ_c exceeding 1 (i.e., on average, subtidal sanctuaries function as sources; Fig. 8). The larger initial population size (Table 1) and enhanced demographic rates (Table 2) relative to other reef types likely allowed subtidal sanctuaries to function as sources. Some subtidal natural and cultch reefs, and even fewer intertidal natural reefs in Pamlico and Core Sounds, served as sources during the May–June time steps (Fig. 8). For the July–August oyster spawning periods, no reef types had a mean λ_c exceeding 1, although infrequently, subtidal sanctuaries, intertidal natural reefs in Core Sound, and hardened shorelines functioned as sources (Appendix S1: Fig. S29). Reefs serving as sources likely exhibited high population sizes (i.e., greater fecundity and associated larval output), enhanced demographic rates (e.g., enhanced survival), and/or ideal
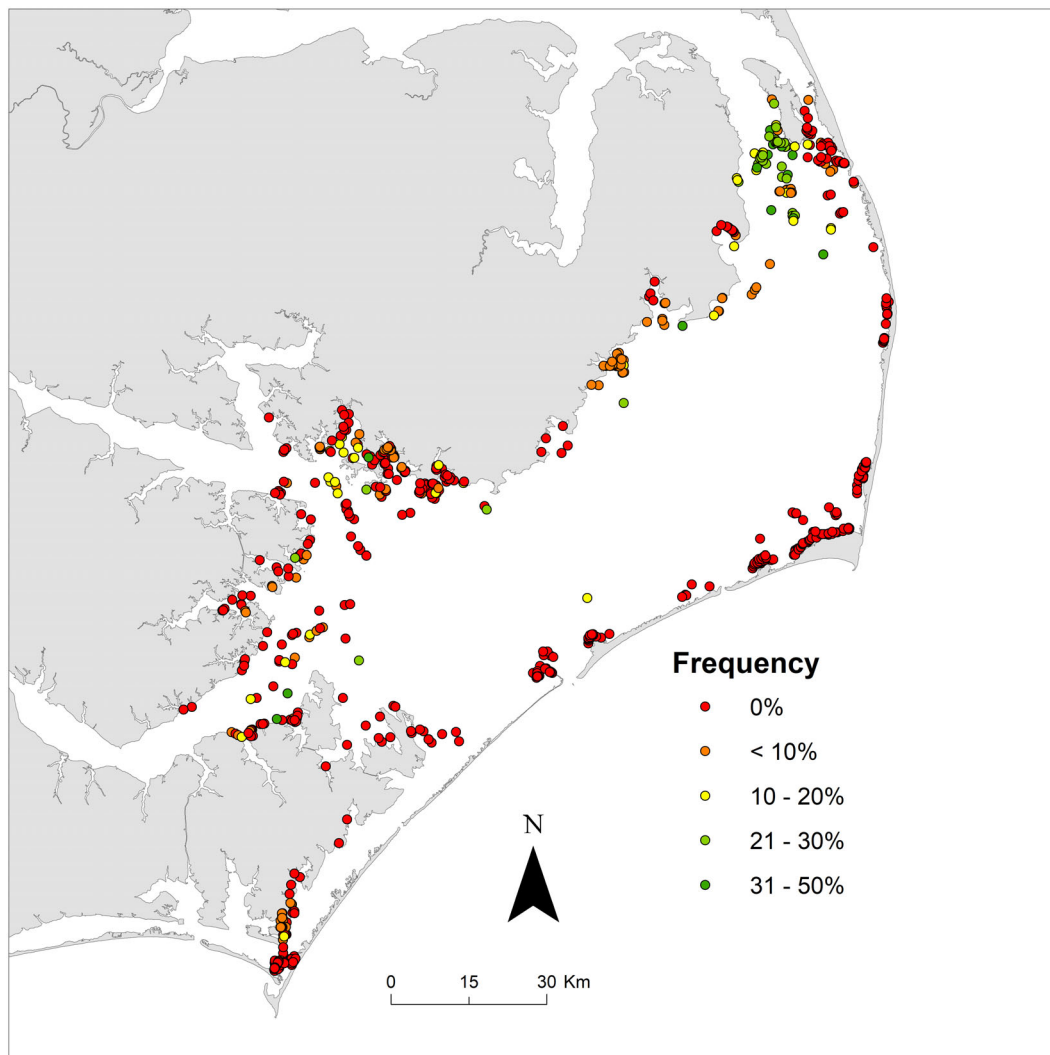
Fig. 9. Frequency of $\lambda_c \geq 1$ at all reefs across the five-year model time frame under the 10% larval mortality d^{-1} scenario. $\lambda_c \geq 1$ indicates a given reef functioned as a source during time t, and $\lambda_c < 1$ indicates a given reef functioned as a sink during time t. Green dots represent frequent source reefs (i.e., $\lambda_c \geq 1$ 31–50% of the time), and red dots represent sink reefs (i.e., $\lambda_c \geq 10$% of the time).

geographic placement (e.g., along dispersal pathways that connected multiple reefs) relative to reefs serving as sinks.

Frequent source reefs (i.e., high frequency of $\lambda_c > 1$ across recruitment events) exhibited greater rates of both larval export and local retention relative to other reefs. For example, for reefs where $\lambda_c > 1$ occurred 50% of the time, ~24% of larvae were exported to other reefs relative to ~18% exported for all reefs, and ~2% of larvae were retained locally relative to ~0.5% retained

locally for all reefs (Tables 4, 5). As frequent source reefs were generally located in the northeastern portion of Pamlico Sound (Fig. 9), it is likely that these reefs are located along dispersal pathways that enhance potential connectivity. The process underlying enhanced local retention for frequent source reefs is unknown; however, hydrodynamic, semi-diurnal seiching within the APES after wind events (Luettich et al. 2002) may reduce dispersal distances in northeastern Pamlico Sound and promote greater local

retention. Further evaluation of the biophysical processes underlying larval export and local retention is warranted. Additionally, while this study provides evidence that reefs throughout Pamlico Sound are well-connected over the scale of multiple years, larval dispersal distances in this system generally range from 1 to 40 km (Puckett et al. 2014, Kroll et al. 2018) such that connectivity may be concentrated in subregions of Pamlico Sound where reefs are concentrated (e.g., southwestern vs. northeastern; Figs. 4–6). Future work using a graph-theoretic approach (sensu Treml et al. 2007) to identify regional graph components, as well as stepping stones that promote sound-wide connection, may be warranted.

Processes underlying oyster metapopulation dynamics and source–sink structure.—Inter-reef larval export substantially impacted metapopulation dynamics relative to local larval retention. Across all reefs, ~18% of larvae originating from a given reef successfully settled on a different reef (Table 4). This value ranged from as high as ~26% for natural subtidal reefs to a low of ~5% for natural intertidal reefs in Core Sound. The geographic distribution of reefs of differing reef types likely contributed to variation in inter-reef larval connectivity. For example, natural subtidal reefs are distributed homogeneously throughout the APES; however, natural intertidal reefs and hardened shorelines are limited to shoreline locations. The magnitude of local retention was lower than inter-reef larval export (e.g., ~0.5% vs. ~18%) due to average dispersal distances (1–40 km) relative to average reef area (0.02 km^2), and likely yielded less impact on metapopulation dynamics. Inter-reef larval connectivity and local retention rates were substantially higher in the present study (~18% and ~0.5%, respectively) than in a previous study that examined inter-reef larval connectivity and local retention of 10 subtidal sanctuaries within the APES (~0.1% and ~0.3%, respectively; Puckett and Eggleston 2016). The elevated inter-reef larval connectivity and local retention rates observed in the present study are due to the inclusion of all known reefs within the system relative to the previous study that included only subtidal sanctuaries (i.e., greater probability of larvae originating from a given reef encountering and settling in a different

reef when connections between all reefs are possible).

Given the high rates of inter-reef larval connectivity relative to local retention observed in the present study, it is probable that larval connectivity is a more important driver of metapopulation dynamics than subpopulation demographics within this system. High levels of inter-reef larval connectivity decouple subpopulation reproduction and recruitment (i.e., reefs are less dependent upon recruitment derived from local retention; Warner and Cowen 2002, Figueira 2009). For example, Figueira (2009) documented a declining importance of demographic rates on metapopulation dynamics at low levels of local retention. Conversely, when local retention is equivalent or greater than larval import from other reefs, subpopulation demographic rates (e.g., growth and survival) are potentially more important drivers of metapopulation dynamics than larval import. However, to quantitatively evaluate the relative importance of (1) within-reef demographics, (2) local retention, and (3) inter-reef larval connectivity on metapopulation dynamics and source–sink dynamics (i.e., λ_c), elasticity analyses are needed and are the subject of ongoing research (Theuerkauf et al., *unpublished data*). Elasticity values represent the proportional contribution of each model parameter to λ_c by assessing how λ_c changes in response to proportional perturbations of model parameters (e.g., increase/decrease by 5%; Puckett and Eggleston 2016).

Although it appears that inter-reef larval connectivity is a more substantial driver of metapopulation dynamics within this system than subpopulation demographic rates, the role of demographics on metapopulation dynamics was still evident. For example, 12 of 14 (86%) subtidal sanctuaries with enhanced growth and survival relative to other reef types served as metapopulation sources. A much lower proportion (7–49%) of other reef types served as subpopulation sources due to reductions in demographic rates (survival and growth) relative to sanctuaries (Table 5). Heightened vertical relief, protection from fishery harvest, and placement within areas of suitable habitat are likely contributing factors to the capacity of subtidal sanctuaries to serve as sources (Lenihan 1999, Schulte et al. 2009,

Puckett and Eggleston 2012, Peters et al. 2017, Puckett et al. 2018). Fishing mortality, reduced vertical relief, and reduced habitat quality likely contribute to the poorer demographic rates of other reef types (Lenihan 1999, Peters et al. 2017).

Caveats regarding model assumptions

Several assumptions were made to simplify the metapopulation model applied in the present study. First, to estimate reef type- and season-specific growth and survival transition probabilities, we averaged oyster density data from all sampling quadrats for a given reef site for each sampling event, and subsequently partitioned density estimates into three size classes. We then pooled these data and applied a linear optimization approach to determine the least-squares estimate for five growth and survival transition probabilities based on size class-specific density data from time t and $t + 1$. This approach allowed for estimation of reef type- and season-specific variation in growth and survival transition probabilities, yet did not allow for variation in transition probabilities within a reef type or season.

Second, distinct proportional daily larval mortality rates: 7.5%, 10%, and 20% d^{-1}, yielded widely varying metapopulation and source–sink dynamic outcomes. Although population trajectories and metapopulation summary statistics under the 7.5% and 20% d^{-1} larval mortality rates are provided (Appendix S1: Figs. S10–S23) to show the range of possible metapopulation outcomes, the 10% proportional daily larval mortality scenario qualitatively aligned with prior field-based observations. Given the impact of this parameter on metapopulation outcomes, further field-based evaluation of proportional daily larval mortality rates within the APES is warranted.

Third, larval dispersal was modeled as passive drift driven solely by surface currents despite evidence that oyster larvae migrate vertically and are generally distributed in the water column according to their ontogenetic stage (Carriker 1951, Dekshenieks et al. 1996, Puckett and Eggleston 2016). Given the well-mixed nature of the APES, it is unclear what water column features oyster larvae might respond to (if any) to regulate their depth, other than a general ontogenetic shift toward deeper depths as sinking speeds exceed swimming speeds (Dekshenieks et al. 1996). In our study system, larval dispersal and connectivity were more sensitive to location and the date of spawning than to larval behavior (Puckett et al. 2014). Including larval behavior may have reduced dispersal distances, thereby increasing local retention, decreasing inter-reef connectivity, and increasing importance of subpopulation demographics ultimately influencing our projection of metapopulation abundance (North et al. 2008, Puckett et al. 2014, Puckett and Eggleston 2016).

Management and broader implications

The present study provides strong evidence for the management of oysters within the APES as an interconnected metapopulation driven largely by inter-reef larval connectivity—larvae were more frequently exported to different reefs than they were retained locally. Thus, oyster restoration and conservation strategies within the APES that focus on creating new reefs in areas that maximize inter-reef connectivity (e.g., Puckett et al. 2018) are likely to be most effective. Subtidal sanctuaries served as the most frequent subpopulation sources to the metapopulation, likely due to a combination of their high subpopulation sizes, enhanced demographic rates, and optimal geographic placement to enhance inter-reef connectivity relative to reefs serving as sinks. Sanctuaries also hosted more stable subadult and adult subpopulations on subtidal sanctuaries, allowing them to remain resilient to periods of reduced recruitment. These findings are consistent with previous studies documenting the value of no-harvest marine protected areas (e.g., Agardy 1994, Botsford et al. 2009, Schulte et al. 2009). Continued protection of subtidal sanctuaries from fishery harvest and construction, or enhancement of additional sanctuaries in areas likely to promote inter-reef connectivity, should be a management priority within this system (e.g., Puckett and Eggleston 2016). Additionally, as some subtidal natural and cultch reefs served as frequent sources to the metapopulation, this study provides evidence of the potential metapopulation source value of fished reefs that should be accounted for in fishery management plans.

Another key finding concerns the importance of the spawning peak in May–June for the oyster metapopulation. Given that overall metapopulation growth rate (λ_M) only exceeded 1 during the

peak primary spawning season (May–June), and was less than 1 during all other model time steps, recruitment failure during May–June could lead to a declining metapopulation if persistent over time (e.g., due to changes in water quality, temperature-induced changes in spawning). Moreover, metapopulation dynamics were very sensitive to larval mortality rate. Future studies should examine the potential impacts of warming oceans, declining pH, and variable salinities on spawning periodicity, larval survival, and overall recruitment success given the relative importance of the May–June spawning period to overall metapopulation dynamics.

Conclusions

The present study applied an empirically based, metapopulation modeling framework to simulate an entire oyster metapopulation to understand underlying source–sink dynamics. The metapopulation appeared too reliant on highly disturbed and harvested natural reefs to persist over time. Efforts to restore (i.e., cultch reefs) and restore + protect (i.e., subtidal sanctuary reefs) have been successful, but likely insufficient in quantity to promote metapopulation persistence. Within the large wind-driven estuary examined in the present study, inter-reef larval connectivity was the major driver of oyster metapopulation dynamics and reef-specific population sizes, demographics, and location appear to jointly determine source–sink status. No-take oyster sanctuaries disproportionately served as metapopulation sources (86% were consistent sources), highlighting the importance of these protected reefs in supporting the metapopulation. Oyster management efforts should aim to protect and restore frequent source subpopulations while managing harvest from sink subpopulations.

ACKNOWLEDGMENTS

LITERATURE CITED

Agardy, M. T. 1994. Advances in marine conservation: the role of marine protected areas. Trends in Ecology and Evolution 9:267–270.

Aiken, C. M., and S. A. Navarrete. 2011. Environmental fluctuations and asymmetrical dispersal: generalized stability theory for studying metapopulation persistence. Marine Ecology Progress Series 428:77–88.

Beissinger, S. R., and M. I. Westphal. 1998. On the use of demographic models of population viability in endangered species management. Journal of Wildlife Management 62:821–841.

Bode, M., L. Bode, and P. R. Armsworth. 2006. Larval dispersal reveals regional sources and sinks in the Great Barrier Reef. Marine Ecology Progress Series 308:17–25.

Botsford, L. W., F. Micheli, and A. Hastings. 2003. Principles for the design of marine reserves. Ecological Applications 13:S25–S31.

Botsford, L. W., J. W. White, M. A. Coffroth, C. B. Paris, S. Planes, T. L. Shearer, S. R. Thorrold, and G. P. Jones. 2009. Connectivity and resilience of coral reef metapopulations in marine protected areas: matching empirical efforts and predictive models. Coral Reefs 28:327–337.

Burgess, S. C., K. J. Nickols, C. D. Griesemer, L. A. K. Barnett, A. G. Dedrick, E. V. Satterthwaite, L. Yamane, S. G. Morgan, J. W. White, and L. W. Botsford. 2014. Beyond connectivity: How empirical methods can quantify population persistence to improve marine protected-area design. Ecological Applications 24:257–270.

Caley, M. J., M. H. Carr, M. A. Hixon, T. P. Hughes, G. P. Jones, and B. A. Menge. 1996. Recruitment and the local dynamics of open marine populations. Annual Review of Ecology and Systematics 27:477–500.

Carriker, M. R. 1951. Ecological observations on the distribution of oyster larvae in New Jersey estuaries. Ecological Monographs 21:19–38.

Carroll, E. L., A. Hall, M. T. Olsen, A. B. Onoufriou, O. E. Gaggiotti, and D. J. Russell. 2020. Perturbation

drives changing metapopulation dynamics in a top marine predator. Proceedings of the Royal Society B: Biological Sciences 287:20200318

Carson, H. S., G. S. Cook, P. C. López-Duarte, and L. A. Levin. 2011. Evaluating the importance of demographic connectivity in a marine metapopulation. Ecology 92:1972–1984.

Castorani, M. C., D. C. Reed, P. T. Raimondi, F. Alberto, T. W. Bell, K. C. Cavanaugh, D. A. Siegel, and R. D. Simons. 2017. Fluctuations in population fecundity drive variation in demographic connectivity and metapopulation dynamics. Proceedings of the Royal Society B: Biological Sciences 284:20162086.

Caswell, H. 2001. Matrix population models. John Wiley & Sons, New York, New York, USA.

Coen, L. D., R. D. Brumbaugh, D. Bushek, R. Grizzle, M. W. Luckenbach, M. H. Posey, S. P. Powers, and S. Tolley. 2007. Ecosystem services related to oyster restoration. Marine Ecology Progress Series 341:303–307.

Cowen, R. K., M. M. Kamazima, S. Sponaugle, C. B. Paris, and D. B. Olson. 2000. Connectivity of marine populations: Open or closed? Science 287:857–859.

Cox, C., and R. Mann. 1992. Temporal and spatial changes in fecundity of eastern oysters, *Crassostrea virginica* (Gmelin, 1791) in the James River, Virginia. Journal of Shellfish Research 11:49–54.

Crowder, L. B., and W. F. Figueira. 2006. Metapopulation ecology and marine conservation. Pages 491–515 *in* J. P. Kritzer, and P. F. Sale, editors. Marine metapopulations. Elsevier, The Netherlands.

Crowder, L. B., S. J. Lyman, W. F. Figueira, and J. Priddy. 2000. Source-sink population dynamics and the problem of siting marine reserves. Bulletin of Marine Science 66:799–820.

Dekshenieks, M. M., E. E. Hofmann, J. M. Klinck, and E. N. Powell. 1996. Modeling the vertical distribution of oyster larvae in response to environmental conditions. Marine Ecology Progress Series 136:97–110.

Dudley, D. L., and M. H. Judy. 1973. Seasonal abundance and distribution of juvenile blue crabs in Core Sound, NC 1965–68. Chesapeake Science 14:51–55.

Epperly, S. P., and S. W. Ross. 1986. Characterization of the North Carolina Pamlico-Albemarle complex. National Oceanic and Atmospheric Administration Technical Memorandum. NMFS-SEFC-175. Washington, D.C., USA.

Esri. 2016. ArcGIS Desktop: Release 10.3. Environmental Systems Research Institute, Redlands, California, USA.

Figueira, W. F. 2009. Connectivity or demography: defining sources and sinks in coral reef fish

metapopulations. Ecological Modelling 220:1126–1137.

Figueira, W. F., and L. B. Crowder. 2006. Defining patch contribution in source-sink metapopulations: the importance of including dispersal and its relevance to marine systems. Population Ecology 48:215–224.

Figueira, W. F., S. J. Lyman, L. B. Crowder, and G. Rilov. 2008. Small-scale demographic variability of the biocolor damselfish, *Stegastes partitus*, in the Florida Keys USA. Environmental Biology of Fishes 81:297–311.

Grabowski, J. H., and C. H. Peterson. 2007. Restoring oyster reefs to recover ecosystem services. Pages 281–298 *in* K. Cuddington, J. E. Byers, W. G. Wilson, and A. Hastings, editors. Ecosystem engineers: plants to protists. Elsevier, The Netherlands.

Haase, A. T., D. B. Eggleston, R. A. Luettich, R. J. Weaver, and B. J. Puckett. 2012. Estuarine circulation and predicted oyster larval dispersal among a network of reserves. Estuarine, Coastal and Shelf Science 101:33–43.

Hanski, I. 1998. Metapopulation dynamics. Nature 396:41.

Holstein, D. M., T. B. Smith, J. Gyory, and C. B. Paris. 2015. Fertile fathoms: deep reproductive refugia for threatened shallow corals. Scientific Reports 5: e12407.

Hughes, T. P., A. H. Baird, E. A. Dinsdale, N. A. Moltschaniwskyj, M. S. Pratchett, J. E. Tanner, and B. L. Willis. 2000. Supply-side ecology works both ways: the link between benthic adults, fecundity, and larval recruits. Ecology 81:2241–2249.

Kennedy, V. S., R. I. E. Newell, and A. F. Eble. 1996. The eastern oyster (*Crassostrea virginica*). Maryland Sea Grant Press, College Park, Maryland, USA.

Kritzer, J. P., and P. F. Sale. 2006. Marine metapopulations. Elsevier, Amsterdam, The Netherlands.

Kroll, I., A. Poray, B. Puckett, D. Eggleston, and J. Fodrie. 2018. Quantifying estuarine-scale invertebrate larval connectivity: methodological and ecological insights. Limnology & Oceanography 63:1979–1991.

Lenihan, H. S. 1999. Physical-biological coupling on oyster reefs: How habitat structure influences individual performance. Ecological Monographs 69:251–275.

Levins, R. 1969. Some demographic and genetic consequences of environmental heterogeneity for biological control. Bulletin of the Entomological Society of America 15:237–240.

Levitan, D. R. 1991. Influence of body size and population density on fertilization success and reproductive output in a free-spawning invertebrate. Biological Bulletin 181:262–268.

Lewis, O., C. Thomas, J. Hill, M. Brookes, T. P. Crane, Y. Graneau, J. Mallet, and O. Rose. 1997. Three ways of assessing metapopulation structure in the butterfly *Plebejus argus*. Ecological Entomology 22:283–293.

Luettich, R. A., S. D. Carr, J. V. Reynolds-Fleming, C. W. Fulcher, and J. E. McNinch. 2002. Semi-diurnal seiching in a shallow, micro-tidal lagoonal estuary. Continental Shelf Research 22:1669–1681.

Mann, R., and D. A. Evans. 1998. Estimation of oyster, *Crassostrea virginica*, larval production and advective loss in relation to observed recruitment in the James River, Virginia. Journal of Shellfish Research 17:239–254.

McMurray, S. E., T. P. Henkel, and J. R. Pawlik. 2010. Demographics of increasing populations of the giant barrel sponge *Xestospongia muta* in the Florida Keys. Ecology 91:560–570.

Mroch III, R. M., D. B. Eggleston, and B. J. Puckett. 2012. Spatiotemporal variation in oyster fecundity and reproductive output in a network of no-take reserves. Journal of Shellfish Research 31:1091–1101.

North Carolina Department of Environmental Quality, Division of Coastal Management. 2012. Estuarine shorelines of NC spatial dataset. Shapefile dataset. https://deq.nc.gov/about/divisions/coastal-management/coastal-management-data/spatial-data-maps ##EstuarineShorelines. Accessed 15 March 2016.

North Carolina Department of Environmental Quality, Division of Marine Fisheries. 2013. Estuarine benthic habitat mapping program. Shapefile dataset. http://portal.ncdenr.org/web/mf/shellfish-habitat-mapping. Accessed 15 Mar 2016.

North, E. W., Z. Schlag, R. R. Hood, M. Li, L. Zhong, T. Gross, and V. S. Kennedy. 2008. Vertical swimming behavior influences the dispersal of simulated oyster larvae in a coupled particle-tracking and hydrodynamic model of Chesapeake Bay. Marine Ecology Progress Series 359:99–115.

Peters, J., D. B. Eggleston, B. J. Puckett, and S. J. Theuerkauf. 2017. Oyster demographics in harvested reefs versus no-take reserves: implications for larval spillover and restoration. Frontiers in Marine Science 4:e326.

Pierson, K., and D. B. Eggleston. 2014. Response of estuarine fish to large-scale oyster reef restoration. Transactions of the American Fisheries Society 143:273–288.

Pietrafesa, L. J., G. S. Janowitz, T. Y. Chao, R. H. Weisberg, F. Askari, and E. Noble. 1986. The physical oceanography of Pamlico Sound. UNC Sea Grant Publication, UNC-WP-86-5, Raleigh, North Carolina, USA.

Planes, S., G. P. Jones, and S. R. Thorrold. 2009. Larval dispersal connects fish populations in a network of marine protected areas. Proceedings of the National Academy of Sciences of the United States of America 106:5693–5697.

Powers, S. P., C. H. Peterson, J. H. Grabowski, and H. S. Lenihan. 2009. Success of constructed oyster reefs in no-harvest sanctuaries: implications for restoration. Marine Ecology Progress Series 389:159–170.

Puckett, B. J., and D. B. Eggleston. 2012. Oyster demographics in a network of no-take reserves: recruitment, growth, survival, and density dependence. Marine and Coastal Fisheries 4:605–627.

Puckett, B. J., and D. B. Eggleston. 2016. Metapopulation dynamics guide marine reserve design: importance of connectivity, demographics, and stock enhancement. Ecosphere 7:6.

Puckett, B. J., D. B. Eggleston, P. C. Kerr, and R. A. Luettich. 2014. Larval dispersal and population connectivity among a network of marine reserves. Fisheries Oceanography 23:342–361.

Puckett, B. J., S. J. Theuerkauf, D. B. Eggleston, R. Guajardo, C. Hardy, J. Gao, and R. A. Luettich. 2018. Integrating larval dispersal, permitting, and logistical factors within a validated habitat suitability index for oyster restoration. Frontiers in Marine Science 5:76.

Pulliam, H. R. 1988. Sources, sinks, and population regulation. American Naturalist 132:652–661.

Rassweiler, A., E. Ojea, and C. Costello. 2020. Strategically designed marine reserve networks are robust to climate change driven shifts in population connectivity. Environmental Research Letters 15:34030.

Reyns, N. B., D. B. Eggleston, and R. A. Luettich. 2007. Dispersal dynamics of postlarval blue crabs, *Callinectes sapidus*, within a wind-driven estuary. Fisheries Oceanography 16:257–272.

Roelofs, E. W., and D. F. Bumpus. 1953. The hydrography of Pamlico Sound. Bulletin of Marine Science 3:181–205.

Schulte, D. M., R. P. Burke, and R. N. Lipcius. 2009. Unprecedented restoration of a native oyster metapopulation. Science 325:1124–1128.

Seward, A., N. Ratcliffe, S. Newton, R. Caldow, D. Piec, P. Morrison, T. Cadwallender, W. Davies, and M. Bolton. 2018. Metapopulation dynamics of roseate terns: sources, sinks and implications for conservation management decisions. Journal of Animal Ecology 88:138–153.

Theuerkauf, S. J., D. B. Eggleston, B. J. Puckett, and K. W. Theuerkauf. 2016. Wave exposure structures oyster distribution on natural intertidal reefs, but not on hardened shorelines. Estuaries and Coasts 40:376–386.

Theuerkauf, S. J., D. B. Eggleston, K. W. Theuerkauf, and B. J. Puckett. 2017. Oyster density and demographic rates on natural intertidal reefs and hardened shoreline structures. Journal of Shellfish Research 36:87–100.

Treml, E. A., P. N. Halpin, D. L. Urban, and L. F. Pratson. 2007. Modeling population connectivity by ocean currents, a graph-theoretic approach for marine conservation. Landscape Ecology 23:19–36.

Warner, R. R., and R. K. Cowen. 2002. Local retention of production in marine populations: evidence, mechanisms, and consequences. Bulletin of Marine Science 70:245–249.

Watson, J. R., B. E. Kendall, D. A. Siegel, and S. Mitarai. 2012. Changing seascapes, stochastic connectivity, and marine metapopulation dynamics. American Naturalist 180:99–112.

Xie, L., and D. B. Eggleston. 1999. Computer simulations of wind-induced estuarine circulation patterns and estuary-shelf exchange processes: the potential role of windforcing on larval transport. Estuarine, Coastal and Shelf Science 49:221–234.

SUPPORTING INFORMATION

Additional Supporting Information may be found online at: http://onlinelibrary.wiley.com/doi/10.1002/ecs2.3573/full